

REVIEW

OTOLITHS OF DEEP WATER FISHES: STRUCTURE, CHEMISTRY AND CHEMICALLY-CODED LIFE HISTORIES

R. W. GAULDIE,* G. COOTE,† K. P. MULLIGAN,‡ I. F. WEST,‡ and N. R. MERRETT§

*Hawaii Institute of Geophysics, University of Hawaii, 2525 Correa Road, Honolulu, HI 96822, U.S.A.;

†Fisheries Research Centre, P.O. Box 297, Wellington, New Zealand; ‡Institute of Nuclear Sciences, Private Bag, Gracefield, Lower Hutt, Wellington; §The Natural History Museum, Cromwell Road, London, SW7 5BD, U.K.

(Received 7 November 1990)

Abstract—1. The gross anatomy and crystalline ultrastructure of the external surfaces has been described for the sagittal otoliths of a 6 million year old fossil otolith and the following bottom-living deep-water teleosts (families in parenthesis): *Coryphaenoides (Nematonurus) armatus* (Macrouridae), *Coryphaenoides (Chalinura) mediterraneus* (Macrouridae), *Cetonus globiceps* (Macrouridae), *Coryphaenoides (Chalinura) leptolepis* (Macrouridae), *Antimora rostrata* (Moridae), *Halosaurus pectoralis* (Halosauridae), *Psychrolutes obesus* and *Neophryrinchthys angustus* (Psychrolutidae).

2. Sections of otoliths were scanned by proton microprobe to yield three dimensional maps of the elemental density of calcium, strontium and, in some otoliths, zinc. The same sections were examined optically for opaque and hyaline zones. For some otoliths, broken sections were examined by SEM and their internal crystalline structure described.

3. The theoretical basis for using cycles in elemental (particularly strontium) composition to interpret life history is examined. Life history information from elemental composition is compared with other information derived both from otoliths and field observations of the species involved.

INTRODUCTION

Deep-water fishes pass their lives in one of the most inaccessible habitats on the planet. They live in a dark, cold environment at depths that we can sample in only a fragmentary way. And yet, whenever we drop baits into even the deepest ocean, fish soon appear; sometimes very large fish when we consider how little apparent sustenance is available at those depths. At depths that one might call moderate—say at 1000 m—that is relatively still, cold and dark, there sometimes occur very large aggregations of fish, for example the orange roughy *Hoplostethus atlanticus* (Gauldie *et al.*, 1989), that seem to occur in numbers quite inappropriate for an organism so far removed from the energy of the sun. These aggregations of deep water fishes are very valuable. For example, each year some 32,000 tonnes of sable fishes are caught around the rim of the Pacific from Japan to California, another 46,000 tonnes of orange roughy are taken off New Zealand, and the Soviet fisheries take at least 7,000 tonnes of blunt-nosed rattail in the North Atlantic and at least 32,000 tonnes of the rough-headed grenadier elsewhere (Merrett, 1989a). How do deep-water fishes spend their lives? Are there well organised, co-adapted communities of fish in the deep (Jumars and Gallagher, 1982; Golovan, 1978); or, are there, as suggested by Haedrich and Merrett (1990) only random assemblages, brought together perhaps by local changes in the density of food? One approach to the solution of this problem lies in the examination of the life history of individual fishes

that is recorded in the chemistry of their otoliths. If such life-history data can be obtained it would provide the biologist with a powerful tool with which to compare the different biochemistries and physiologies of fishes. Comparisons that ought to provide much of the basic information about both the population structure and abundance of fishes.

Otoliths are calcium carbonate concretions found in the endolymphatic sac of most teleost fish. Otoliths are usually formed from the aragonite morph of calcium carbonate (Degens *et al.*, 1969), but other morphs of calcium carbonate, vaterite and calcite, also occur as complete, or partial, replacements of aragonite in some otoliths. Mixed, or non-aragonitic, otoliths occur in varying proportions in different species ranging from less than 1% up to 20% of otoliths sampled (Strong *et al.*, 1986, Gauldie, 1991).

Otoliths have been widely used in ageing fish. Most otolith ageing studies have utilised what are thought to be annual patterns either in the deposition of protein, or different crystalline ultrastructure (Six and Horton, 1977), but it is now possible to determine the ages and growth patterns of fish through the use of daily increments in otoliths. Daily growth increments have been demonstrated in the hard parts of many organisms (Neville, 1967). Daily microincrements have been described in detail in the otoliths of fish by Panella (1971). Since Panella's description, many studies have dealt with daily increments in the otoliths of wild and captive reared fish. Many tagging studies used in conjunction with tetracycline injection have demonstrated the daily nature of

microincrement deposition in fish (e.g. Laurs *et al.*, 1985). Physiological mechanisms for microincrement deposition have been investigated suggesting that both calcium mobilisation (Mugiya, 1987) and neuroprotein secretion are involved (Gauldie and Nelson, 1988). Although it was originally suspected microincrement disposition might be aperiodic, or even cease, after sexual maturity (Ralston and Miyamoto, 1983), other studies indicate that in some species daily microincrementation occurs over most of the life of the fish (Ralston and Williams, 1988; Pulfrich and Griffiths, 1988; Gauldie *et al.*, 1989).

In addition to age, otoliths also carry information about the growth rate of the fish (Radtke *et al.*, 1985) in their ultrastructure, and information about the temperature of their environment in their chemistry (Radtke, 1984; Gauldie *et al.*, 1986). Under normal physiological conditions otoliths, unlike bone, are not resorbed and recrystallised thereby providing a stable chemical and ultrastructural record. Resorption of the otolith may occur under certain circumstances including extreme stress (Mugiya and Uchimura, 1989). However for most of the life of most fish otolith material is generally thought to be stable, providing a permanent record of the patterns of change in chemistry and crystal structure of the otolith.

Otoliths have been used to age deep-water fishes using both conventional annual check ring methods (Gordon and Duncan, 1985) and daily growth increment based techniques (Ralston and Williams, 1988). Daily increment techniques have been used in orange roughy ageing and have revealed the possibility that some deep water fishes may have k-selection-biased life history strategies (Gauldie *et al.*, 1989). Otoliths from the deep water macrourid *Coryphaenoides guentheri* recovered from 1880 to 1950 m depth showed macro- and microincrement structures similar to those in other teleosts (Rannou and Thiriott-Quvreux, 1975), suggesting that the same range of periodic phenomena are recorded in the ultrastructure of otoliths of deep sea fishes as are recorded in the otoliths of shallow water species.

However, the otoliths of oreos from about 1100 m showed a number of crystalline complexities that made both the macro- and microincrement structures of the otoliths difficult to discern (Davies *et al.*, 1988). Complex (multi-check-ring), and polycrystalline (different sized crystals) otoliths ought to be the rule rather than the exception in deep water fishes because of the increase in the solubility of carbon dioxide with cold and pressure. Increase in solubility of carbon dioxide increases the pH and decreases saturation

with respect to calcium carbonate. A combination of pH and pressure effects result in variations in the 'compensation depth' at which carbonates will dissolve more readily than they precipitate. In the North Atlantic the compensation depth is between 5000 and 6000 m, and between 4000 and 5000 m in the South Pacific (Sverdrup *et al.*, 1942). The effects of pressure and pH on carbon dioxide solubility also result in a shift in the stability of the aragonite morph of calcium carbonate towards calcite (which is the thermodynamically most stable morph) with depth. Aragonite saturation with respect to calcite falls to about 25% at 1000 m and less than 5% at 2000 m in the Pacific, and 25% at 1400 m and 5% at 5000 m in the Atlantic (Li *et al.*, 1969). Oreo otoliths recovered from 1100 m deep (Pacific Ocean) remained aragonitic, although with complex crystal structures consisting of blocks of disordered, atactic crystals (Davies *et al.*, 1988) stabilized in the aragonite morph presumably by their protein matrix. The very existence of aragonite otoliths in the bicarbonate buffered endolymphatic sac of depth water fishes implies a significant metabolic cost in overcoming the decreasing pH gradient due to pressure and depth.

Other components of otolith chemistry such as strontium content, are known to be preferentially associated with aragonite deposition (Zeller and Wang, 1956; Oxburgh *et al.*, 1959). Other elements, particularly zinc, are associated with aragonites that have low strontium levels (Odum, 1957; Gauldie *et al.*, 1980). In this study we have described the variation in crystalline structure of otoliths from deep-water bottom-living fishes of both the North Atlantic and Pacific as well as describing the variation in the strontium, and in some cases, zinc chemistry. In addition, we examined the ultrastructure and chemistry of a fossil otolith for any indications of specific diagenetic effects on aragonite crystals that may parallel depth effects. The biological significance of the chemical and ultrastructural variation in the otolith was assessed in terms of other otolith features, depth, field studies of the species involved, and the probable physiological, chemical and crystallographic causes that control the observed variation in the strontium chemistry of otoliths.

MATERIALS AND METHODS

Sagittal otoliths were taken from a number of deep water species from the North Atlantic and South Pacific Oceans. Species and depth from which the samples were taken are shown in Table 1. Species

Table 1.

Species	Mean depth of capture (m)	Sulcus/otolith ratio	Opaque zone count	Strontium peak count	Anti-sulcus crystal width (μm)	Sulcus crystal width
<i>Antimora rostrata</i>	1872	0.28	15	10	0.83	6.48
<i>Coelorinchus labiatus</i>	1533	0.22	17/9	9	—	4.93
<i>Centoneurus globiceps</i>	1477	0.19	20	15+	3.68	6.90
<i>Coryphaenoides mediterraneus</i>	1975	0.19	6	6	1.00	2.12
<i>Coryphaenoides armatus</i>	4800	0.18	9	—	1.02	1.29
<i>Trachyrincus murrayi</i>	1300	0.18	25+	12-14	—	10.00
<i>Coryphaenoides leptolepis</i>	4090	0.13	23/12	12	1.00	1.21
<i>Halosaurus pectoralis</i>	1000	0.13	—	—	10.00	4.54
<i>Neophrynichthys angustus</i>	1000	0.12	—	—	—	—
<i>Psychrolutes obesus</i>	1000	0.03	—	—	—	2.06

names for some species are undergoing revision and the older genus name is shown in parenthesis after the newer genus name where appropriate.

The fossil otolith was supplied by the New Zealand Geological Survey of the Department of Scientific and Industrial Research. The otoliths were collected from the Temian horizon of the Wairarapa (New Zealand) formation, stratigraphically dated at about 6 million years old.

Otoliths were mounted on aluminium pin mounts with epoxy resin. Where more than one otolith (or a pair of otoliths) was available, one was mounted sulcus side up, and the other sulcus side down. After examination of the whole otolith, they were broken by thumb pressure across the dorso-ventral axis of the otolith and the broken sections mounted with epoxy resin on aluminium pin subs. One fossil otolith was broken and mounted this way. The otoliths on pin stubs were sputter coated with gold and photographed with a Philips 505 scanning electron microscope.

Broken sections of pin mounted otoliths were then polished and scanned with a proton microprobe following the method described by Coote *et al.* (1982). A fossil otolith was mounted on a glass slide with epoxy resin and ground down to the nucleus, and scanned by the proton microprobe and photographed by SEM. Prior to microprobe scanning, mounted otoliths were photographed by reflected light.

Otolith sections were scanned at 50 µm intervals with the proton microprobe resulting in up to a 400 × 400 orthogonal scan matrix.

Graphical analysis and smoothing of the microprobe scan data was carried out using the LOWESS routine of the 'S' statistical package (Cleveland, 1979). The LOWESS technique shows graphically the underlying functional relationship between variables (in this case elemental composition and distance on the surface of the otolith) without having to fit the data to an *a priori* parametric function. Calcium counts were very high in comparison to strontium counts and the variation in calcium count could often be better displayed by moving the 'floor' of the trace from 0 to some arbitrary level that would emphasize the variation in calcium counts rather than total counts.

Otolith anatomical nomenclature generally follows Pannella (1980), general aragonite crystal terminology follows Carricker *et al.* (1983) and specific internal otolith structures use the terms in Gauldie (1988a, 1990). In some instances, structures in the form of particular organisations of crystals appear that are not readily translatable into the standard nomenclature. Attention will be drawn to such structures as and when they arise in the results section to avoid adding to the lengthy discussion. In other cases, there are examples of otolith nomenclature in the literature that are not sufficiently general to warrant use, for example, 'outer face' has no meaning for flatfish, and

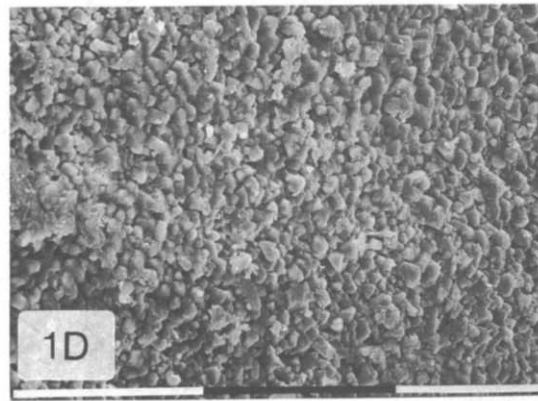
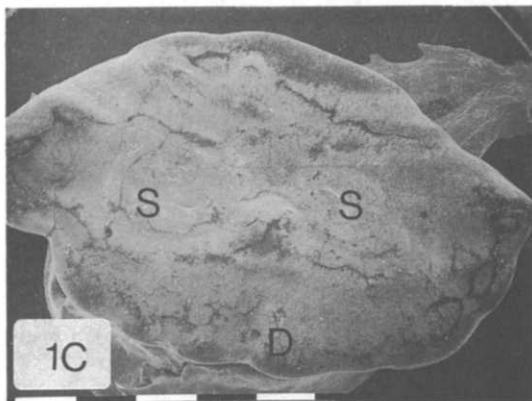
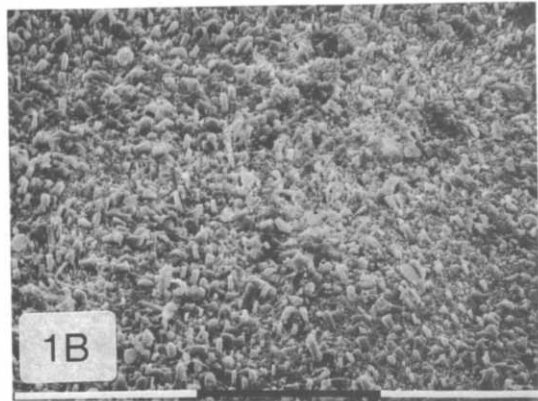
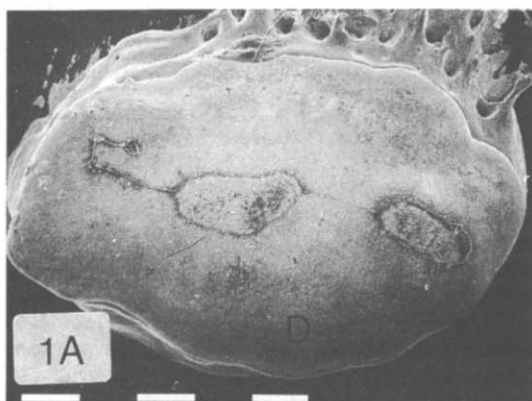


Fig 1 (A)-(D). *Caption overleaf*

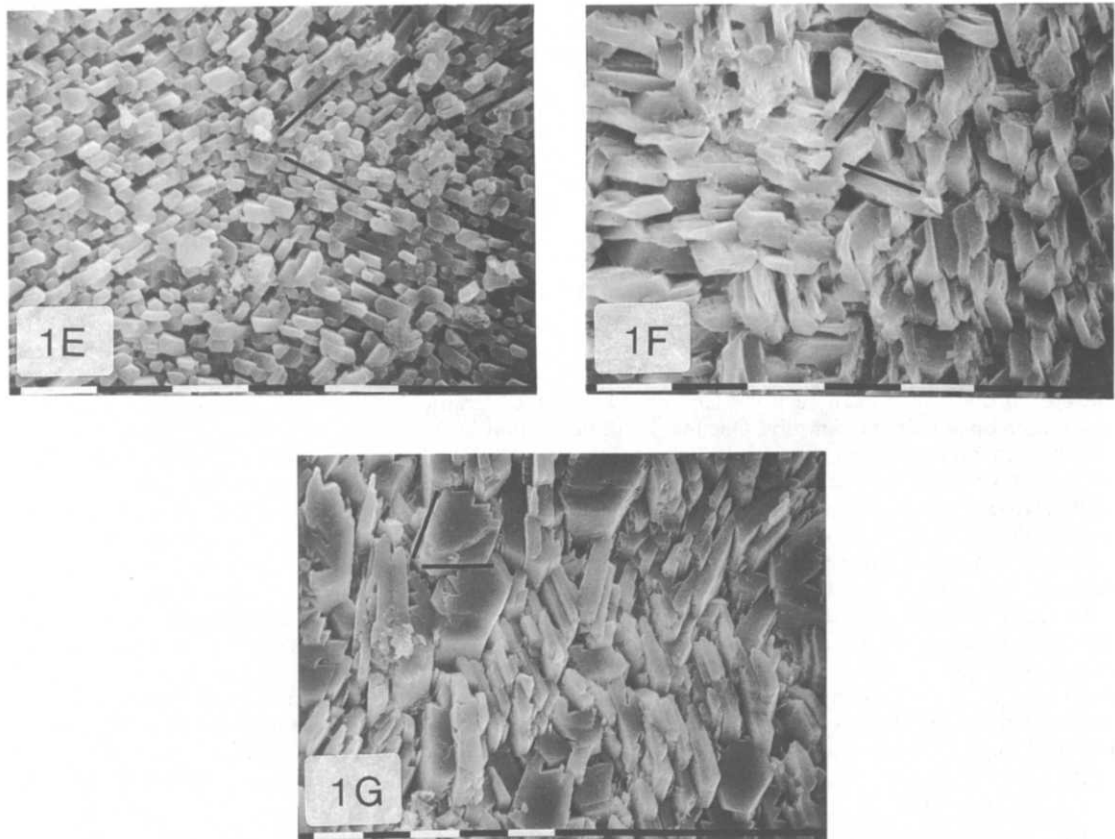


Fig. 1 (E)-(G)

Fig. 1. (A) The anti-sulcus surface of the otolith of *Cetonurus globiceps* was smooth with a weakly scalloped dorsal (D) edge. The bar is 1 mm. (B) The crystals of the anti-sulcus surface of the otolith had the form of monoclinic needles projecting from the surface, interspersed with small crystals. The bar is 0.1 mm. (C) The sulcus surface of the otolith reflected the weakly scalloped dorsal (D) edge and had a shallow, wide sulcus (S). The bar is 1 mm. (D) The crystals at the edge of the sulcus surface were in the form of uniform and closely packed crystals of uniform thickness. The bar is 0.1 mm. (E-G) The crystals of the sulcus surface changed progressively in width and organisation towards the sulcus (E, F) having a massive block-like appearance in the sulcus itself (G). The crystals in E-G all show the 64° twinning angle. The bar in E-G is 10 μ m.

in these cases a more general term is introduced, e.g. anti-sulcus surface for 'outer face' and the older term introduced in parenthesis. Size is given as head length (HL), forklength (FL) or total length (TL).

RESULTS

The ultrastructural and chemical data of otoliths have been grouped by species. Some discussion of the crystalline and chemical features has been included in the results section to facilitate the discussion section of the paper. In our assessment of the usefulness of otoliths to deep-water, bottom-living fish life history studies we have examined the sulcus and anti-sulcus surfaces for crystalline characteristics that may be associated with the depth of capture because the crystals at the surface of the otolith are the ones being deposited at the time (and consequently depth) of capture. Broken section of otoliths have been used to examine the variation in crystallinity and chemistry during the development of the otolith.

Although there were significant differences between species in the morphology of macrourid otoliths, there

is, in the context of this study, sufficient similarity to make illustrations of every otolith redundant. The otolith morphology of *Cetonurus globiceps* is shown in detail and the morphology of the otoliths of other macrourids is illustrated only when indicated by a marked departure from the type illustrated by *C. globiceps*.

Cetonurus globiceps (*Macrouridae*)

Cetonurus globiceps is distributed throughout the North Atlantic over a range of soundings from 1200 to 2500 m. The specimens whose otoliths were used in this study were caught between 1450 and 1505 m.

The anti-sulcus surface (outer face) of the otolith of *C. globiceps* was smooth, weakly scalloped but without a dorso-ventral ridge (Fig. 1A). The crystals of the anti-sulcus surface have a well defined lath-like appearance, but no indications (Fig. 1B) of being organized around the 64° twinning angle reported for otolith aragonite crystals (Gauldie and Nelson, 1988).

The sulcus surface (inner face) of the otolith of *C. globiceps* is very smooth with a very poorly defined

sulcus (Fig. 1C). The sulcul surface of the otolith showed a range in the habit of what were otherwise well defined crystals of aragonite. Crystals at the edge of the otolith were closely packed with few interstices evident between crystals (Fig. 1D). Within the general area of the sulcul groove the crystal structure and organization changed from lath-like

projections (Fig. 1E), through to a crystalline mat (Fig. 1F) to a block-like habit (Fig. 1G) at the deepest part of the sulcus (colliculum). All of the crystals in Fig. 1E, F, G were organised around the 64° twinning angle. The differences in size of crystals from the sulcul and anti-sulcul surfaces are shown in Table 1.

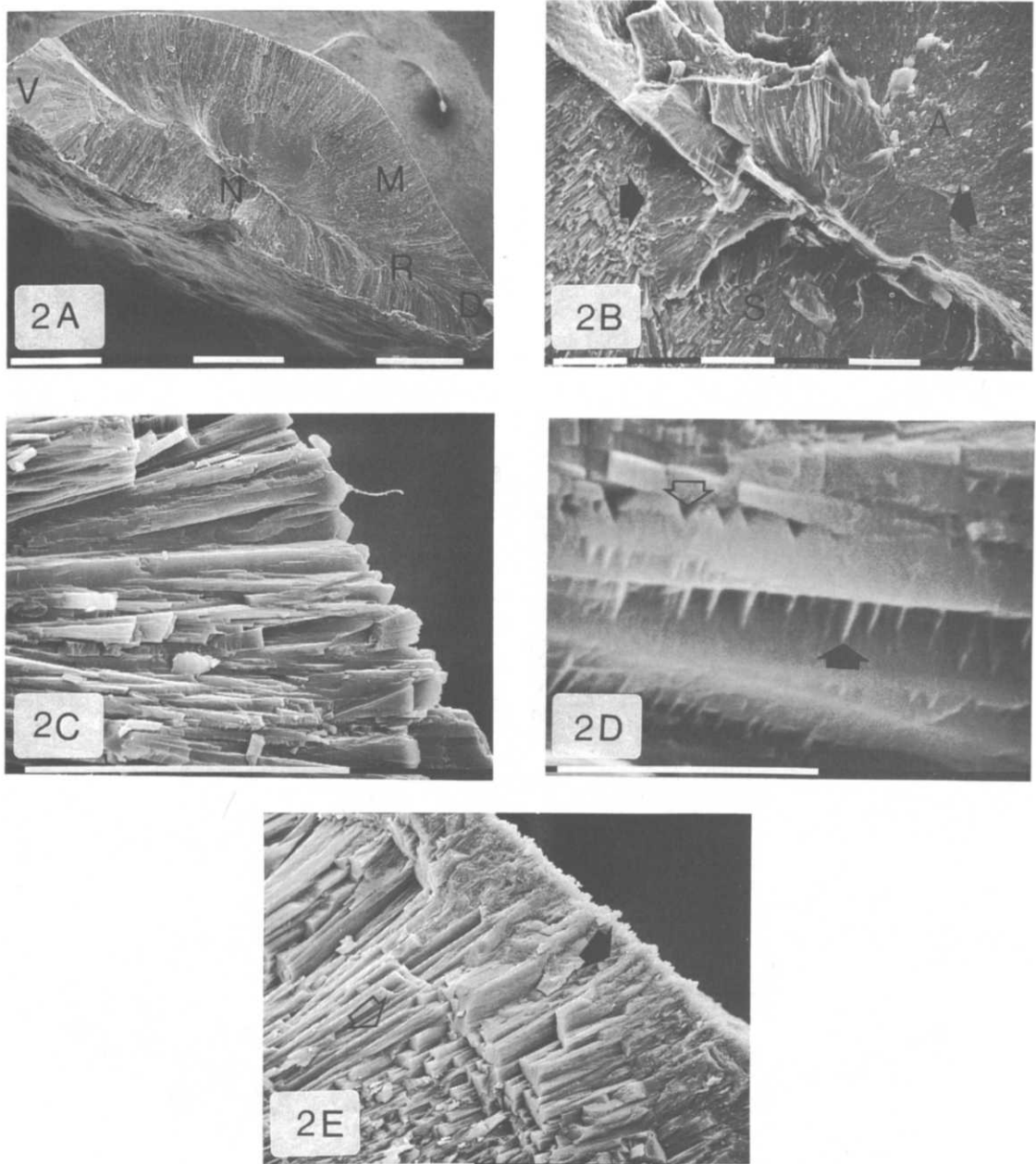


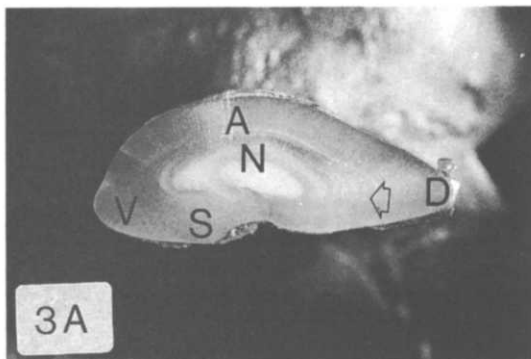
Fig. 2. (A) A section of the otolith of *Cetonura globiceps* broken along the dorso-ventral (D, V) growth axis showed a primordium around the nucleus (N) with a long radial twin crystal (R) along the dorsal growth axis with shorter medial twin crystals (M) growing out to the sulcul and anti-sulcul surfaces of the otolith. The bar is 1 mm. (B) Detail of the primordium showed a well-defined boundary (arrows) between the primordium and the crystals of the sulcus side (S) of the otolith, as well as the finer crystals of the anti-sulcus (A) side. The bar is 0.1 mm. (C) Detail of the sulcus side showed wide crystals growing out to the sulcus edge. The bar is 0.1 mm. (D) At higher magnifications, the wide crystals of the sulcus side of the otolith showed cross-braced (arrows) and notched (open arrows) crystals. The bar is 10 μm . (E) Some parts of the anti-sulcus surface showed a tendency for large crystals within the otolith (open arrows) to develop into a finer crystals (arrows) at the anti-sulcus surface. The bar is 0.1 mm.

A section of the otolith of *C. globiceps* broken along the dorso-ventral axis showed a well defined primordium surrounding the nucleus and a well defined dorso-ventral growth axis passing through the nucleus (Fig. 2A). Detail of the primordium showed the crystalline material of the sulcus close to the nucleus, as well as the difference in crystal size between the anti-sulcus and sulcus parts of the otolith (Fig. 2B). The anti-sulcus part of the otolith was much larger than the sulcus part (Fig. 2A). The otolith showed well defined epitaxial growth along the growth axes with a long radial twin crystal growing to the edge with shorter medial twins growing to the anti-sulcus and sulcus surfaces (Fig. 2A). The crystals of the sulcus part of the otolith were quite wide (Fig. 2C) with a cross-bracing structure appearing to cross between crystals (Fig. 2D). Some parts of the anti-sulcus surface showed a tendency for wider crystals to become progressively modified into much finer crystals at the surface (Fig. 2E).

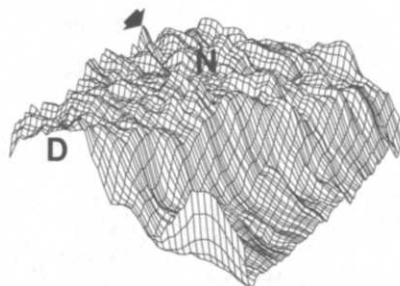
When the broken surface of the otolith of *C. globiceps* was polished and photographed by reflected light a number of optical features appeared that were not visible in the broken section. A series

of opaque and hyaline zones could be seen along the main growth axes of the otolith with sharp drop in opacity (i.e. white by reflected light) at about a quarter of the distance from the nucleus to the dorsal edge (Fig. 3A). There were about 20 distinguishable opaque zones along the dorsal axis, most of which were very closely spaced compared to other otoliths. The anti-sulcus part of the otolith and a number of evenly spaced narrow opaque zones (Fig. 3A). The sulcus side of the otolith was separated from the anti-sulcus side by a refractive boundary and the sulcus part of the otolith showed no visible opaque and hyaline zone structure (Fig. 3A).

A proton microprobe scan of the strontium surface of the sectioned otolith of *Cetonus globiceps* showed a very complex surface with only a slightly heightened strontium level along the sulcus surface (Fig. 3B). Anastomosing ridges of strontium occurred in succession along the dorsal segment with less well defined ridges along the ventral segment. There were up to 15 strontium ridges along the dorsal segment, the far edge of which was not covered by the microprobe. A calcium scan with the trace floor set at zero showed a fairly featureless structure with weak dorso-



Sr *Cetonus globiceps* CGLO scan453



View from NW. Aspect ratio is 1. Maximum value is 140. Floor is 0

3B



View from NW. Aspect ratio is 1. Maximum value is 20520. Floor is 0

3C



View from NW. Aspect ratio is 1. Maximum value is 20520. Floor is 15000

3D

Fig. 3. (A) A polished dorso-ventral (D, V) section of the otolith of *Cetonus globiceps* showed an opaque (white by reflected light) core around the nucleus (N) with decreasing opacity along the dorso-ventral growth axis. The anti-sulcus (A) part of the otolith contained a number of opaque and hyaline zones. A refractive boundary (arrow) separated the sulcus (S) part of the otolith. The bar is 1 mm. (B) The strontium surface of the otolith showed an anastomosing series of ridges with only a weak (arrow) peak in strontium at the sulcus. There were up to 15 ridges between the slight depression at the nucleus (N) and the cut off dorsal (D) edge. (C) The calcium surface was tilted from the anti-sulcus (high) to sulcus (low) edge. (D) Raising the floor of the calcium surface emphasised the tilt but also showed a series of more-or-less parallel ridges running from the anti-sulcus to sulcus edge.

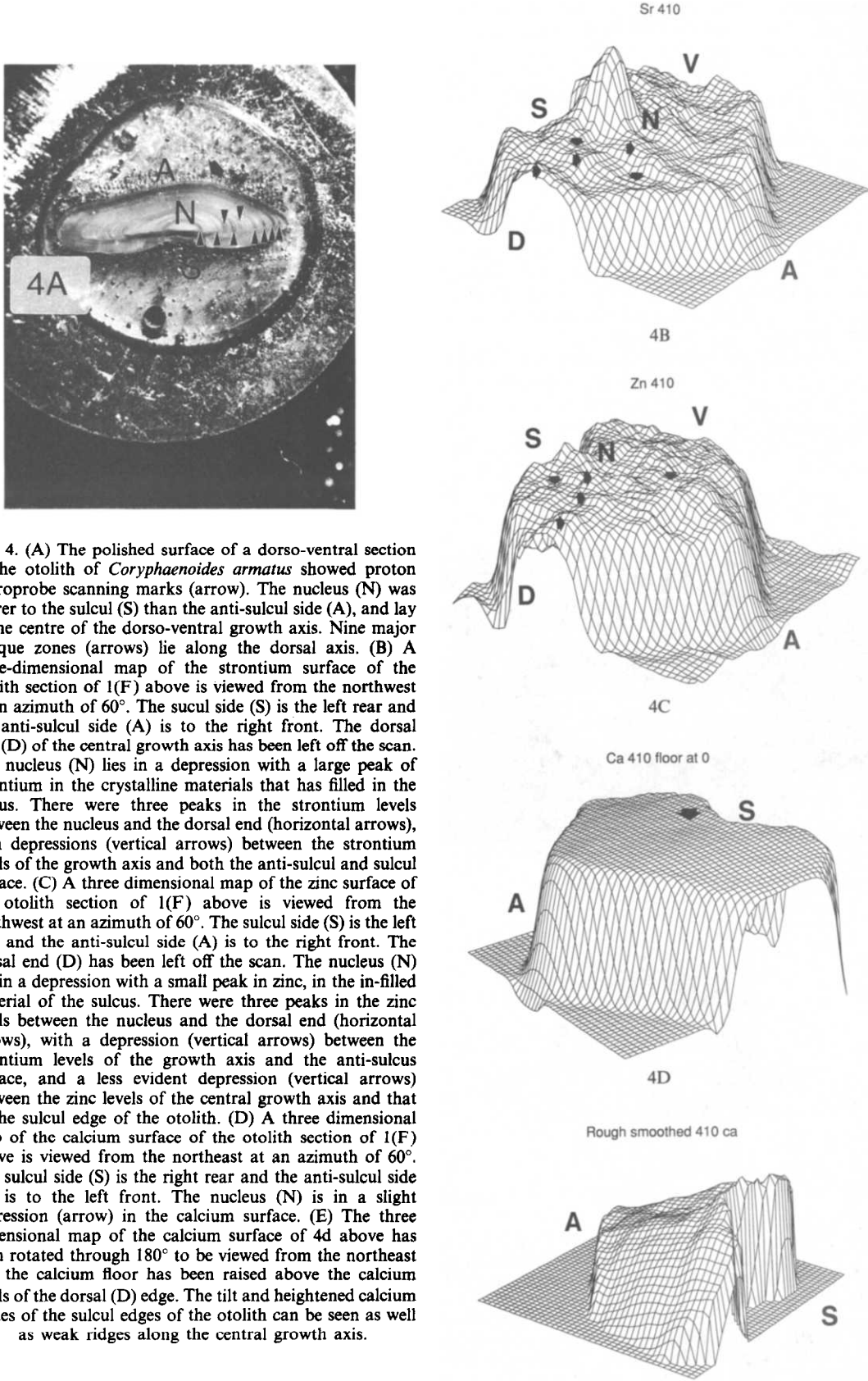


Fig. 4. (A) The polished surface of a dorso-ventral section of the otolith of *Coryphaenoides armatus* showed proton microprobe scanning marks (arrow). The nucleus (N) was nearer to the sulcus (S) than the anti-sulcus side (A), and lay at the centre of the dorso-ventral growth axis. Nine major opaque zones (arrows) lie along the dorsal axis. (B) A three-dimensional map of the strontium surface of the otolith section of 1(F) above is viewed from the northwest at an azimuth of 60°. The sulcus side (S) is the left rear and the anti-sulcus side (A) is to the right front. The dorsal end (D) of the central growth axis has been left off the scan. The nucleus (N) lies in a depression with a large peak of strontium in the crystalline materials that has filled in the sulcus. There were three peaks in the strontium levels between the nucleus and the dorsal end (horizontal arrows), with depressions (vertical arrows) between the strontium levels of the growth axis and both the anti-sulcus and sulcus surface. (C) A three dimensional map of the zinc surface of the otolith section of 1(F) above is viewed from the northwest at an azimuth of 60°. The sulcus side (S) is the left rear and the anti-sulcus side (A) is to the right front. The dorsal end (D) has been left off the scan. The nucleus (N) lies in a depression with a small peak in zinc, in the in-filled material of the sulcus. There were three peaks in the zinc levels between the nucleus and the dorsal end (horizontal arrows), with a depression (vertical arrows) between the strontium levels of the growth axis and the anti-sulcus surface, and a less evident depression (vertical arrows) between the zinc levels of the central growth axis and that of the sulcus edge of the otolith. (D) A three dimensional map of the calcium surface of the otolith section of 1(F) above is viewed from the northeast at an azimuth of 60°. The sulcus side (S) is the right rear and the anti-sulcus side (A) is to the left front. The nucleus (N) is in a slight depression (arrow) in the calcium surface. (E) The three dimensional map of the calcium surface of 4d above has been rotated through 180° to be viewed from the northeast and the calcium floor has been raised above the calcium levels of the dorsal (D) edge. The tilt and heightened calcium values of the sulcus edges of the otolith can be seen as well as weak ridges along the central growth axis.

View from SE. Aspect ratio is 1. Maximum value is 169939. Floor is 150000

ventral ridges (Fig. 3A). Raising the floor of the calcium scan increases resolution resulting in an apparent ridge of increased calcium counts along the anti-sulcul edge of the calcium surface and showed a series of ridges in the dorsal segment paralleling those in the strontium surface (Fig. 3d), but were too weakly defined to count.

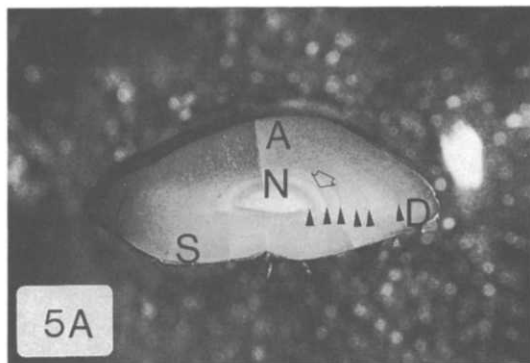
Coryphaenoides (Nematonurus) armatus (Macro-uridae)

Coryphaenoides armatus is one of the most widely distributed macrourids throughout the world's oceans. The otolith described here came from a specimen caught at 4800 m in the North Atlantic, where the overall observed sounding range is 2172–5400 m.

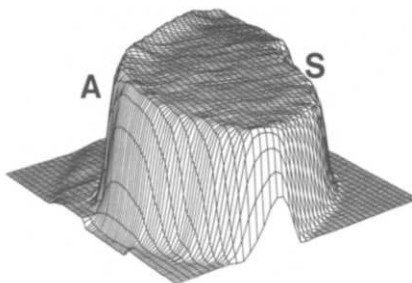
The anti-sulcul surface of the otolith of *C. armatus* was smooth with very little surface sculpturing that was limited to a weakly defined series of ridges radiating from the nucleus part of the sulcus towards the edge of the otolith. Within the sulcus, lath-like aragonite crystals projected at right angles at the sulcus surface of the otolith. Outside of the sulcus,

towards the edge of the surface of the otolith was less lath-like, and was similar to the anti-sulcul surface with a tendency for crystals to be grouped at the 64° twinning angle.

An otolith of *C. armatus* was sectioned along the dorso-ventral axis and polished. The surface was scanned by a proton microprobe for calcium, strontium and zinc. The scanned otolith is shown by reflected light in Fig. 4A. Tracks left by the proton microprobe can be seen on the surface of the otolith but they do not obscure the pattern of light and dark zones of the otolith. The nucleus of the otolith is closer to the sulcul surface than it is to the anti-sulcul surface of the otolith and the principal growth axes from the nucleus to the edges of the otolith are very close to the sulcul surface in comparison to the otoliths of other species. The anti-sulcul part of the otolith showed an opaque zone structure, and the intersection of those zones with the central growth axes had the same appearance as the zones found in the central growth axes of otoliths of other species. There were nine major opaque zones along the dorsal axis of the otolith. Opaque zones have been used

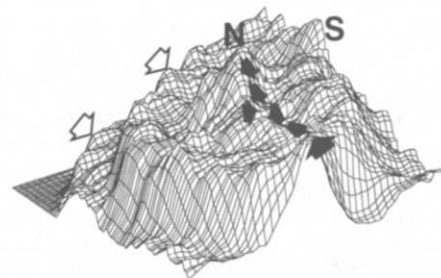


Ca *Coryphaenoides mediterranea* CMED scan456

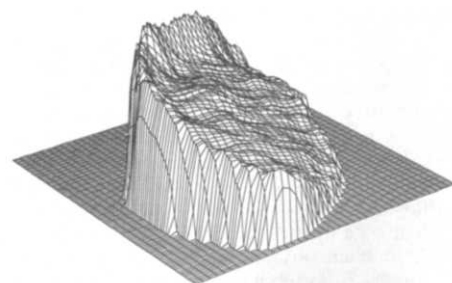


View from NE. Aspect ratio is 1. Maximum value is 17948. Floor is 0

Sr *Coryphaenoides mediterranea* CMED scan456



Ca *Coryphaenoides mediterranea* CMED scan456



View from NE. Aspect ratio is 1. Maximum value is 17948. Floor is 13000

Fig. 5. (A) A polished dorso-central (D, V) section through the nucleus (N) of the otolith of *Coryphaenoides mediterraneus* showed a strongly-refractive surface with an opaque (i.e., white by reflected light) core that decreases in opacity along the dorso-ventral axis. There was a refractive change (open arrow) between the anti-sulcul (A) and sulcus (S) part of the otolith. A succession of opaque zones were visible along the dorso-ventral growth axis (arrow). The bar is 1 mm. (B) The strontium surface showed peaks at the nucleus (N) and sulcus (S), dropping in two distinct steps to the edge of the otolith. Each of the steps contain apparent ridges of higher strontium counts (arrows). Six ridges of increased strontium count could be discerned (closed arrows) along the nucleus to dorsal edge growth axis. (C) The calcium surface of the otolith shows higher counts at the anti-sulcul (A) than the sulcus (S) edge. (D) Raising the floor of the calcium surface showed a series of weakly defined ridges of increased calcium counts running more-or-less in parallel from the anti-sulcul to sulcus surface.

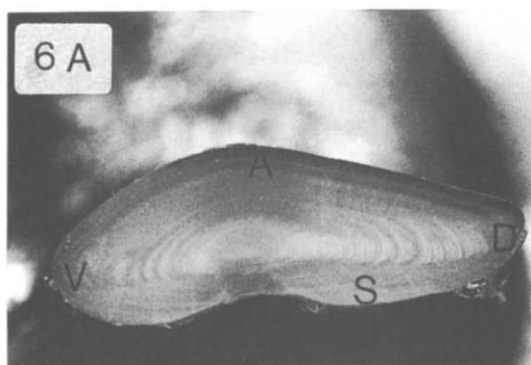
to estimate age in many fish species and 'age' estimated from opaque zones counts as well as 'age' estimated from cycles in strontium content are shown in Table 1 for all of the sectioned otoliths reported in this study except *C. armatus* because the micro-probe trace failed to reach the dorsal extremity of the otolith. The otolith had a distinct nucleus and the sulcus was filled in with crystalline materials consequently forming a very shallow groove compared to the sulcus of the otoliths of other species (Fig. 4A).

A three dimensional map of the strontium concentration of the surface of a dorso-ventral section of the otolith of *C. armatus* is shown in Fig. 4B. The nucleus lies in a depression in the strontium surface (Fig. 4B). The crystalline material deposited in the apex of the sulcus (colliculum) showed a large peak in strontium (Fig. 4B). SEM pictures of the otolith surface showed a marked change in crystalline structure between the crystals of the sulcus surface of the otolith and the material in the sulcus itself, in which the sulcus contained much larger crystals compared to the crystals on the rest of the sulcus surface of the otolith. The differences in size between crystals of the sulcus and the anti-sulcus surface are shown in Table 1. The rest of the strontium surface showed a heightened

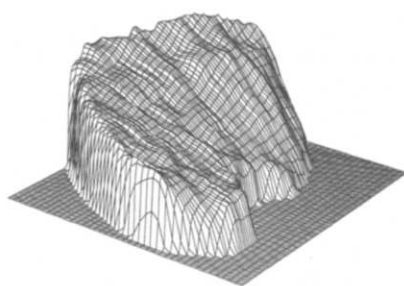
level in the strontium level in the central growth axes of the otolith that pass through the nucleus that was separated by a shallow depression in strontium level between both the anti-sulcus and sulcus surfaces of the otolith (Fig. 4B). A series of 4–5 peaks in strontium occurred along the central growth axes between the nucleus and the edges of the otolith.

A three dimensional map of the zinc concentration of the surface of the dorso-ventral section of the otolith of *C. armatus* is shown in Fig. 4C. The zinc surface showed a depression in zinc content at the nucleus (Fig. 4C). The zinc content of the crystal material in the sulcus was higher than the rest of the otolith, but not as markedly as for strontium (Fig. 4C). The zinc surface showed a series of 4–5 peaks along the central growth axis that had a similar pattern to the strontium peaks. However, the rest of the surface showed a number of dissimilarities to the strontium surface. The zinc levels of the sulcus and anti-sulcus edges are only weakly separated from the central growth axes.

Calcium counts were high, values of almost 170,000 compared to 1100 for strontium and 600 for zinc. The high count levels compared to the variation



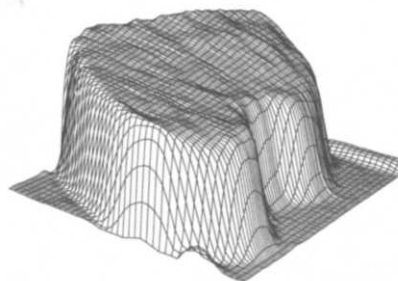
Ca *Coryphaenoides leptolepis* CLEP scan447



View from NW. Aspect ratio is 1. Maximum value is 10676. Floor is 7000

6C

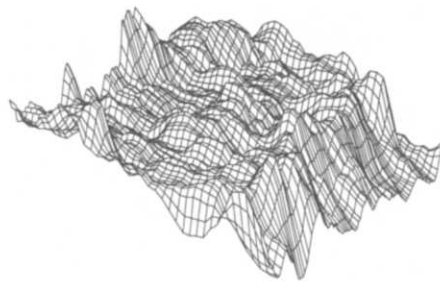
Ca *Coryphaenoides leptolepis* CLEP scan447



View from NW. Aspect ratio is 1. Maximum value is 10676. Floor is 0

6B

Sr *Coryphaenoides leptolepis* CLEP scan447



View from NW. Aspect ratio is 1. Maximum value is 126. Floor is 0

6D

Fig. 6. (A) A polished dorso-ventral section through the nucleus of the otolith of *Coryphaenoides leptolepis* showed an opaque (i.e. white by reflected light) centre with a series of opaque and hyaline zones along the dorso-ventral (D, V) axis. The refractive line divides the otolith into an anti-sulcus (A) part and a sulcus (S) part. There were more opaque and hyaline zones in the anti-sulcus than sulcus part of the otolith. The bar is 1 mm. (B) The calcium surface showed a shallow sulcus and a tilt from high (anti-sulcus) to low (sulcus). (C) Raising the floor of the calcium counts emphasized the tilt, but also showed a series of more-or-less parallel ridges of calcium running from the sulcus to anti-sulcus surface. (D) The strontium surface showed a central ridge of higher strontium counts running along the dorso-ventral growth axis intersected by a series of weakly defined ridges.

in calcium counts effectively flatten the calcium surface unless the scale is expanded (Fig. 4D). Scale expansion was achieved by raising the 'floor' of the three dimensional map. For the calcium content of the surface of the dorso-ventral section of the otolith of *C. armatus* is shown in Fig. 4E, the 'floor' was raised from 0 to 150,000 giving a maximum count of 16,994 from the new zero level. The calcium surface that results is unlike the strontium and zinc surfaces in that it is strongly tilted with higher calcium levels along the sulcus edge of the section and lower calcium levels along the anti-sulcus edge of the sections (Fig. 4E). There is a depression in calcium at the nucleus (Fig. 4E) with an apparently marked decline in calcium along the dorsal central growth axes (Fig. 4E), but not along the other growth axis (Fig. 4E). A number of ridges appeared in the calcium surface but were too weakly defined to count.

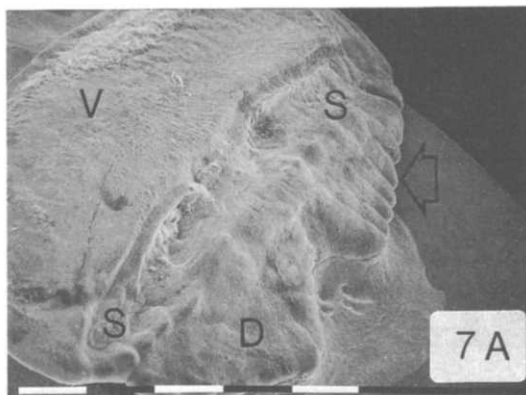
Coryphaenoides (Chalinura) mediterraneus (Macro-uridae)

Coryphaenoides mediterraneus is distributed in deep water in the Mediterranean and North Atlantic

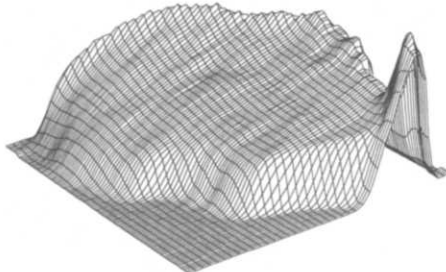
(North Atlantic observed range 1272–2645 m soundings). The otoliths described here came from a specimen caught between 1940 and 2010 m in the North Atlantic.

The anti-sulcus surface of the otolith showed a weak dorso-ventral groove and a lobed, rather than scalloped edge. The otolith is longer along the anterior-posterior axis, than *C. armatus*. The crystalline organization of the anti-sulcus surface gave the appearance of disordered aggregation, but in places some of the crystals appeared to be organized around the 64° twinning angle.

The sulcus surface was dominated by shallow, wide sulcus. Outside of the sulcus, the sulcus surface consisted of many monoclinal crystals orthogonal to the sulcus surface, but without any indication of organization around any angular, or other, orientation. Within the sulcus, the crystals were also orthogonal to the surface, but had the appearance of aragonitic laths. Both the surfaces outside and within the sulcus indicated a rough deposition surface with wide interstices between crystals that penetrate deep into the otolith. The differences in size between

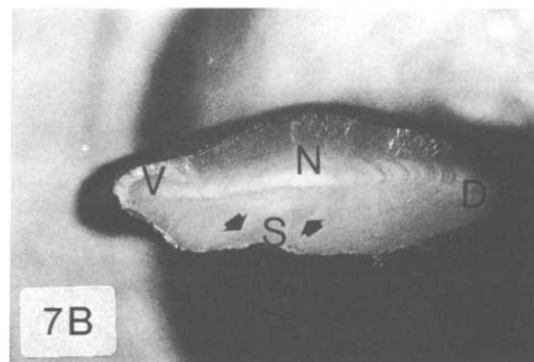


Ca Coelorinchus labiatus CLAB scan.444

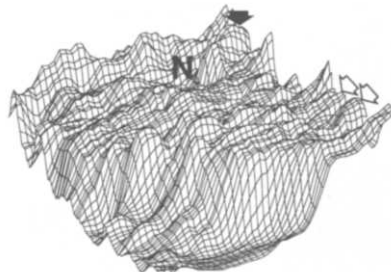


View from NE. Aspect ratio is 1. Maximum value is 10593. Floor is 0

7C



Sr Coelorinchus labiatus CLAB scan.444



View from NE. Aspect ratio is 1. Maximum value is 122. Floor is 0

7D

Fig. 7. (A) The sulcus side of the otolith of *Coelorinchus labiatus* showed a deep sulcus (S) dividing the otolith into a broad ventral (V) part and a narrow dorsal part with a lobed edge (arrows). The bar is 1 mm. (B) A polished section along the dorso-ventral (D, V) axis of the otolith showed an opaque (i.e. white by reflected light) core with a succession of opaque and hyaline zones along the dorso-ventral growth axis. The change in refractive index of the crystalline material (arrows) that fill the sulcus emphasizes the asymmetry of the sulcus (S) and nucleus (N). The bar is 1 mm. (C) The calcium surface of the otolith section had a marked tilt from the anti-sulcus (high) to sulcus (low) edge. There is a peak corresponding to the ventral edge of the otolith. (D) The strontium surface of the otolith section showed a complex pattern of more-or-less parallel ridges and intermittent peaks (open arrows). There was a strontium peak in the infilled sulcus (arrow) and a depression at the nucleus (N).

crystals in the sulcus and those on the anti-sulcus surface are shown in Table 1.

A broken section along the dorso-ventral axis of *C. mediterraneus* showed a relatively simple otolith organization. Epitaxial growth of crystals occurred along the dorso-ventral growth axis with twinned crystals resulting in a long medial twin from the nucleus to the edge of the otolith, and two shorter twins leading to the anti-sulcus and sulcus surfaces respectively (Fig. 4A). The crystal epitaxis showed crystal twinning to centre at the nucleus, but there was very little indication of a sulcus, either in terms of a depression in the otolith or in terms of any difference in internal crystal structure. The medial crystal twins were almost orthogonal to the sulcus surface, but, surprisingly they were also orthogonal to the anti-sulcus surface even though there were clear differences in the crystalline structure at both surfaces. The anti-sulcus part of the otolith was much wider than the sulcus part resulting in the growth axes (and nucleus) being closer to the sulcus surface than they were to the anti-sulcus surface. The crystalline appearance of the otolith was uniform and (apart of the obvious crystal epitaxis) almost featureless with only a few traces of weak crystalline anomalies in the dorsal section of the sulcus part of the otolith.

The broken dorso-ventral section through the nucleus of the otolith of *C. mediterraneus* was polished and showed a strongly refractive surface in which a dorso-ventral growth axis passed through the

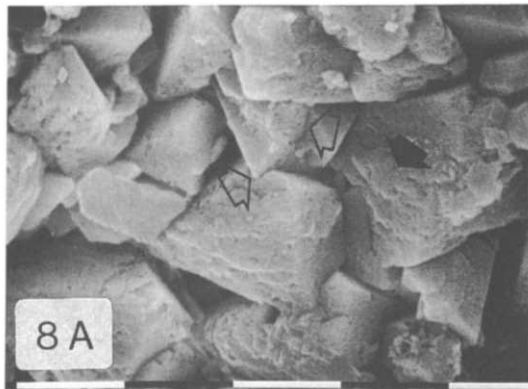
nucleus with a succession of opaque and hyaline zones with decreasing opacity (white by reflected light) from the nucleus (Fig. 5A). Six major zones could be counted along the dorsal growth axis.

A proton microprobe scan of the strontium surface of the otolith of *C. mediterraneus* showed a very complex surface (Fig. 5B). Two major peaks in strontium occurred, one at the nucleus and one at the sulcus. A ridge of higher strontium counts runs down the central growth axes (i.e. the dorso-ventral axes) separated by shallow grooves from higher strontium counts at the sulcus and anti-sulcus edges of the otolith. Six ridges of higher strontium counts could be discerned along the nucleus to dorsal growth axis.

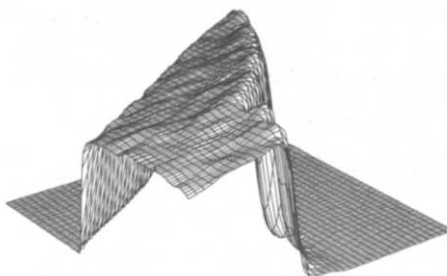
A calcium scan at floor zero of the *C. mediterraneus* otolith showed an anti-sulcus lip in the calcium ion counts surface (Fig. 5C). Raising the floor to 13,000 counts increases emphasis on the anti-sulcus calcium lip and also shows more structure in calcium count surface of the otolith (Fig. 5D). The calcium structure behaves inversely of that of the strontium surface; with higher calcium and lower strontium counts along the anti-sulcus edge and the reverse for the sulcus edge. A series of ridges appeared in the calcium surface but were too weakly defined to count.

Coryphaenoides (Chalinura) leptolepis (Macrouridae)

This is a North Atlantic species with a sounding range of 1884 to 4787 m. The specimen

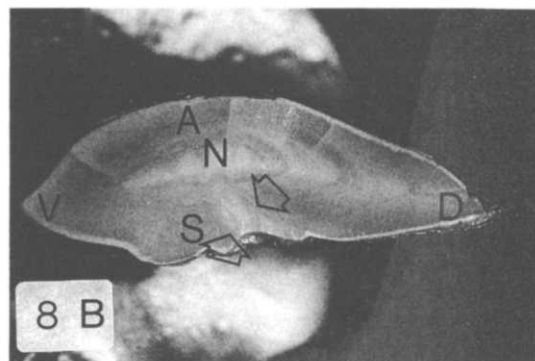


Ca Trachyrincus murrayi TMUR scan462 far end

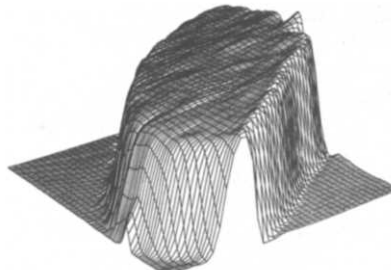


View from SW. Aspect ratio is 1. Maximum value is 15726. Floor is 0

8C(i)



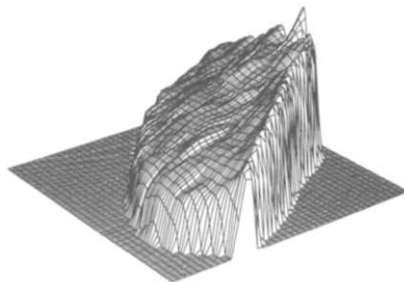
Ca Trachyrincus murrayi TMUR scan459 near end



View from SW. Aspect ratio is 1. Maximum value is 17476. Floor is 0

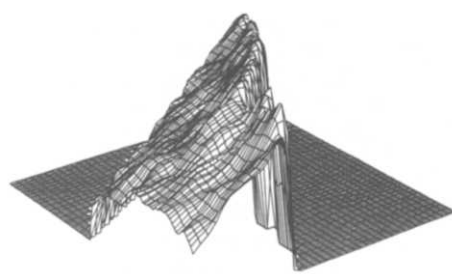
8C(ii)

Fig. 8 (A)-(C). Caption overleaf

Ca *Trachyrincus murrayi* TMUR scan459 near end

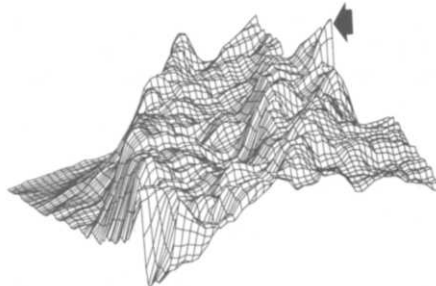
View from SW. Aspect ratio is 1. Maximum value is 17478. Floor is 11000

8D(i)

Ca *Trachyrincus murrayi* TMUR scan462 far end

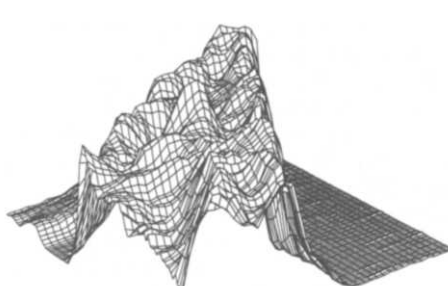
View from SW. Aspect ratio is 1. Maximum value is 15726. Floor is 11000

8D(ii)

Sr *Trachyrincus murrayi* TMUR scan459 near end

View from SW. Aspect ratio is 1. Maximum value is 192. Floor is 0

8E(i)

Sr *Trachyrincus murrayi* TMUR scan462 far end

View from SW. Aspect ratio is 1. Maximum value is 152. Floor is 0

8E(ii)

Fig. 8. (A) At higher magnification the aragonite blocks of the sulcus show pits (arrows) and twinning between crystals (open arrows). The bar is 10 μm . (B) A polished section along the dorso-ventral (D, V) axis of the otolith showed an opaque (white by reflected light) core around the nucleus (N) with opaque and hyaline zones in the anti-sulcul (A) and sulcul (S) parts of the otolith as well as the dorso-ventral axis. The change in refractive index of the crystalline material that has filled in the sulcus (arrows) showed the asymmetry between the nucleus and the sulcus. The bar is 1 mm. (C) The calcium surface showed a tilt in the reverse direction with increased counts at the sulcus edge. The otolith section was scanned as two separate halves (i) and (ii). (D) Raising the floor of the calcium surface emphasised the sulcus calcium ridge and showed calcium peaks at the sulcus edge. The otolith section was scanned as two separate halves (i) and (ii). (E) The strontium surface showed heightened counts along the dorso-ventral (D, V) growth axis. Strontium peaks occurred along both the sulcus and anti-sulcus edge with peaks (arrow) at the sulcus itself. The otolith section was scanned as two separate halves (i) and (ii).

used in this study was caught between 4080 and 4100 m.

The anti-sulcus surface of the otolith of *C. leptolepis* was smooth with slight ridges at the edges of the otolith. The crystals of the anti-sulcus surface had the appearance of disorganized laths growing orthogonal to the surface.

The sulcus was shallow with few surface features. The crystal structure of the sulcus surface consisted of a mixture of aragonite blocks and laths growing orthogonal to the surface. The differences in size of crystals from the sulcus and anti-sulcus surfaces are shown in Table 1.

A polished dorso-ventral section of the otolith of *C. leptolepis* showed a complex structure when viewed by reflected light. The otolith showed a well defined dorso-ventral growth axis dividing the otolith into a larger anti-sulcus and smaller sulcus part (Fig. 6A). The dorso-ventral growth axis showed a series of opaque and hyaline zones similar to those of other macrourids; an additional series of opaque and hyaline zones occurred in

both the sulcus and anti-sulcus parts of the otolith (Fig. 6A). There were more opaque and hyaline zones in the anti-sulcus part of the otolith than in the sulcus part (Fig. 6A). Although the sulcus appeared as a flattened groove in the whole otolith, the dorso-ventral section showed that the sulcus had been progressively filled in with crystalline material (Fig. 6A). Depending on whether opaque zones are counted singly, or as groups, there were between 23 (single) and 12 (grouped) opaque zones in the dorsal growth axis.

The calcium surface of the section of *Coryphaenoides leptolepis* showed the shallow sulcus typical of the otolith and a tilted appearance with calcium higher on the anti-sulcus side (Fig. 6B). Raising the calcium floor emphasized the tilt of the surface but also showed additional structures: a weak ridge running along the central growth axis and further ridges running more-or-less parallel from the anti-sulcus to sulcus surface (Fig. 6C).

The strontium surface of the section of *Coryphaenoides leptolepis* showed a number of

features similar to those of the calcium surface: a central ridge of higher strontium counts running along the dorso-ventral growth axes, intersected by a series of weakly defined ridges (Fig. 6D). Strontium counts in the sulcus itself were slightly higher than in the immediate area, but not significantly higher than peaks in other areas of the otolith (Fig. 6D). The scanned area does not cover the whole surface so that it was not possible to count the number of strontium peaks along the dorsal axis.

Coelorinchus labiatus (Macrouridae)

Coelorinchus labiatus in the North Atlantic occurs over the observed sounding range 785–1900 m. The sample for which this otolith was drawn was caught between 1494 and 1572 m.

The otolith of the *Coelorinchus* species was very different in structure from the otoliths of the rattail genus *Coryphaenoides*. The otolith had a well developed sulcus dividing in the otolith into a larger, smooth ventral section, and a smaller dorsal section

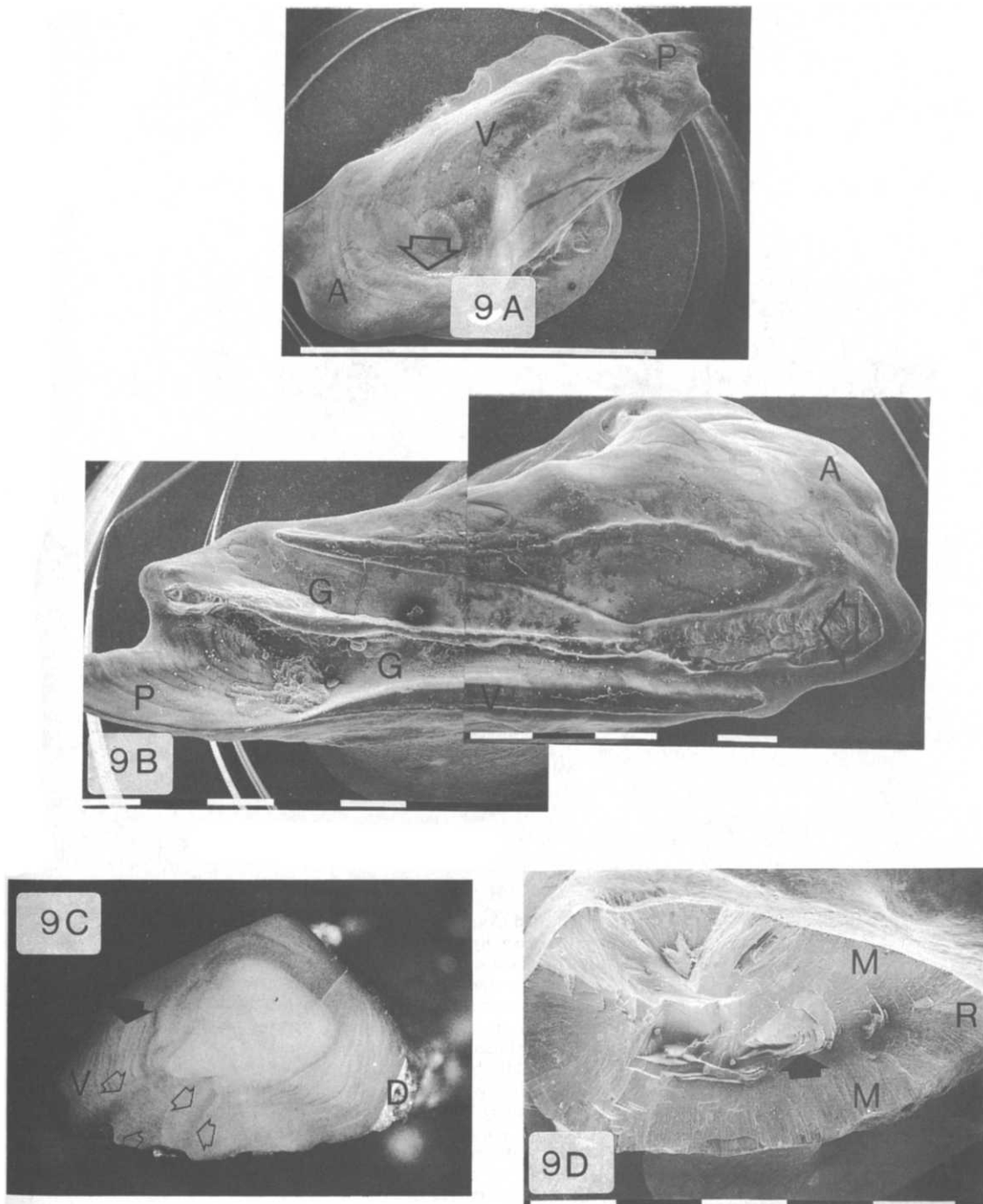


Fig. 9 (A)–(D). *Caption overleaf*

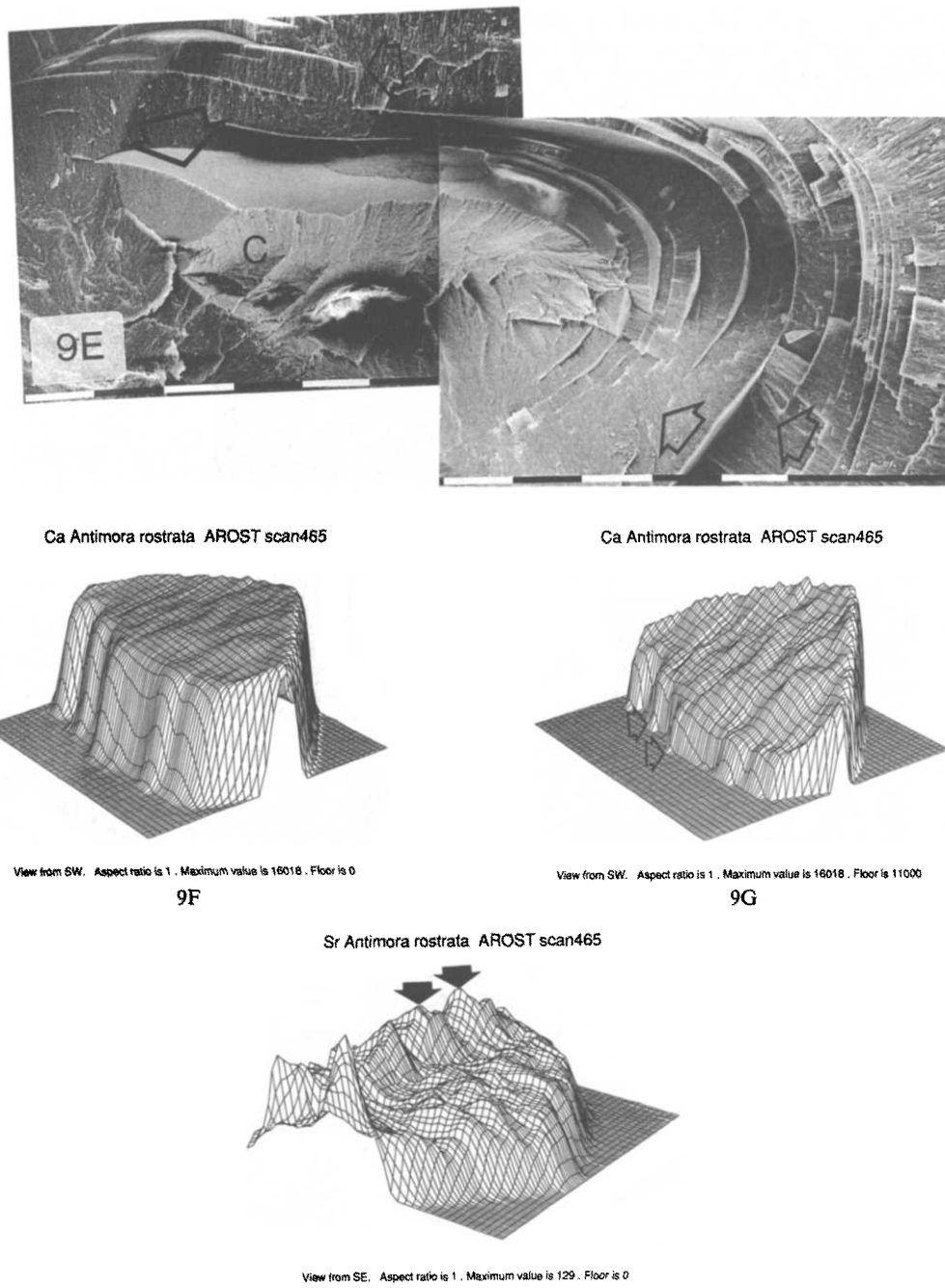


Fig. 9. (A) The otolith of *Antimora rostrata* was elongated along the antero-posterior (A, P) axis with a long ventral (V) edge and dorsal (D) lobe. The anti-sulcus surface was generally smooth, but a coarsely crystalline cleft (arrows) was on the apex of the dorsal lobe. The bar is 10 mm. (B) The sulcus surface of the otolith was complex with sulcus-like grooves (both marked G) running antero-posteriorly (A, P). At the anterior end of the otolith there was a further depressed and pitted area (arrow). The bar is 1 mm. (C) A polished dorso-ventral (D, V) section of the otolith of *Antimora rostrata* showed an opaque (white by reflected light) core surrounded by many fine opaque lines (arrows) especially on the dorso-ventral axis. Optical changes in the sulcus part of the otolith suggest that two sulci (open arrows) have been filled in with crystalline material. The bar is 1 mm. (D) A broken section of the otolith showed epitaxial growth with a longer radial (R) and shorter medial (M) crystals. Spalling lines (arrows) were visible. The bar is 1 mm. (E) At higher magnifications, the smooth surface (arrow) and incomplete penetration (open arrow) of spalling lines could be seen. One spalling line showed an almost orthogonal shift in its plane of growth (curved arrow), but not in its internal crystal structure (C). The bar is 0.1 mm. (F) The triangular shape of the otolith section can be seen in the calcium surface with a number of grooves corresponding to the structure of the sulcus. (G) Raising the floor of the calcium surface showed a tilt in the usual anti-sulcus (high) to sulcus (low) direction as well as parallel ridges (arrows) running from the anti-sulcus (high) to sulcus (low) edge. (H) The strontium surface showed a series of peak (arrows) in the strontium counts in the filled-in sulcus of the otolith, and running from the anti-sulcus to sulcus edge across a groove of low strontium.

with a well developed prismatic structure (Fig. 7A). Prismatic refers to the development of bounded growth axes which is the common form of growth in many molluscs (Wilber and Saleuddin, 1983) and otoliths of most fish species (Morales-Nin, 1987). The crystals of the surface of the ventral half were organized around the 64° twinning angle. The crystals of the dorsal end of the sulcus surface had a block-like crystal organization, becoming more monoclinic and organised along the 64° twinning angle within the sulcus. The difference in size between crystals from the sulcus and anti-sulcus surfaces are shown in Table 1.

A section of the otolith of *C. labiatus* broken along the dorso-ventral axis showed epitaxial growth along the dorso-ventral axis with a long radial twin crystal with medial twins each of about the same length. The anti-sulcus and sulcus parts of the otolith were of similar size, more-or-less symmetrically deposited around the central growth axis. The nucleus and the sulcus showed a degree of asymmetry with the sulcus slanting away from the nucleus becoming located about a third of the way between the nucleus and the dorsal edge of the otolith. When the surface of the otolith section was polished opaque and hyaline zones could be seen along the dorso-ventral growth axis (Fig. 7B). The sulcus was displaced from the nucleus, but there was an angled line of refractive material that showed where the sulcus had been progressively filled in with crystalline material (Fig. 7B). A series of opaque and hyaline zones were laid down in both the sulcus and anti-sulcus parts of the otolith (Fig. 7B). Depending on whether opaque zones were treated as occurring singly or in groups, there were either 17 (single) or 9 (grouped) opaque zones along the dorsal growth axis.

The calcium surface of the section of *C. labiatus* had a marked tilt from the anti-sulcus to sulcus edge with a distinct lip along the anti-sulcus edge (Fig. 7C). The calcium scan showed a marked peak at the end of the ventral growth axis that corresponds to the markedly crystalline material visible in Fig. 7B at the ventral end of the otolith.

The strontium surface of the section of *C. labiatus* showed a complex pattern of ridges running more-or-less in parallel between the sulcus and anti-sulcus edge of the otolith (Fig. 7D). The sulcus showed an increased strontium count right on the sulcus edge with intermittent peaks in strontium between the sulcus edges and the nucleus of the otolith (Fig. 7D). There were at least nine identifiable ridges in strontium counts along the dorsal axis.

Trachyrincus murrayi (*Macrouridae*)

Trachyrincus murrayi is a North Atlantic species that has been caught in soundings ranging from 1010 to 1884 m. The otoliths used in this study came from a specimen caught between 1280 and 1344 m.

The anti-sulcus surface of the otolith of *T. murrayi* was relatively featureless with an amorphous crystalline appearance. The anti-sulcus surface showed a wide but shallow sulcus. The crystals of the anti-sulcus surface showed a projecting lath-like structure organized at the 64° twinning angle, with the interstices between laths penetrating deep into the otolith.

Within the sulcus, the crystal surface was formed of a pavement of block-like aragonite crystals. At higher magnifications the aragonite crystals of the sulcus showed a pitted surface and twinning insertion between individual crystals (Fig. 8A). The differences in size between crystals from the sulcus and anti-sulcus surfaces are shown in Table 1.

A section of the otolith of *T. murrayi* broken along the dorso-ventral axis showed epitaxial growth along the dorso-ventral axis with a long radial twin and medial twins of about the same length going to the anti-sulcus and sulcus surfaces of the otolith. The sulcus was displaced away from the nucleus towards the dorsal edge. When the dorso-ventral section was polished a series of opaque and hyaline zones were visible along the dorso-ventral growth axis with weaker zones continuing into both the sulcus and anti-sulcus parts of the otolith (Fig. 8B). The polished section showed a change in optical appearance between the crystals of the filled-in part of the sulcus and those in the rest of the otolith (Fig. 8B). There were both wide and narrow opaque and hyaline zones along the dorsal axis but resolution was poor and the total number difficult to count. However, counting the individual zones visible suggested, without grouping, about 25 or more opaque zones.

The otolith of *T. murrayi* was too large to deal with as a single scan and was scanned as two slightly over-lapping halves.

Calcium scans of the sectioned otolith of *T. murrayi* showed a reversal in the calcium tilt with increased calcium counts along sulcus rather than the anti-sulcus edge of the otolith (Fig. 8C). Raising the floor of the calcium counts emphasized the development of the sulcus calcium ridge and showed marked calcium peaks at the sulcus edge (Fig. 8D).

Strontium scans showed heightened counts at both the anti-sulcus and sulcus edges with a central ridge of higher strontium counts running more-or-less along the central dorso-ventral growth axis (Fig. 8E). Strontium peaks occurred at the sulcus edge but they were not significantly higher than other peaks in the strontium surface (Fig. 8E). Strontium peaks showed a regular pattern along both the sulcus and anti-sulcus edges, but the marked central ridge may have served to obscure the pattern of more-or-less parallel ridges of heightened strontium that run from the sulcus to anti-sulcus edges in other otoliths (Fig. 8E). Counting peaks in strontium was difficult because of the overlaying problem but between 12 and 14 ridges could be counted along the dorsal axis.

Antimora rostrata (*Moridae*)

Antimora rostrata has a pandemic distribution down to about 3000 m soundings. The otolith used in this study came from a specimen caught between 1815 and 1930 m in the North Atlantic.

Seen from the anti-sulcus surface, the otolith of *A. rostrata* was elongated, tapering towards the posterior end (Fig. 9A). The anti-sulcus surface showed a number of radiating ridges along the ventral side of the otolith with a dorsal lobe at the anterior end (Fig. 9A). The apex of the anti-sulcus surface was pitted, with a coarse crystalline texture (Fig. 9A). Most of the anti-sulcus surface of the otolith

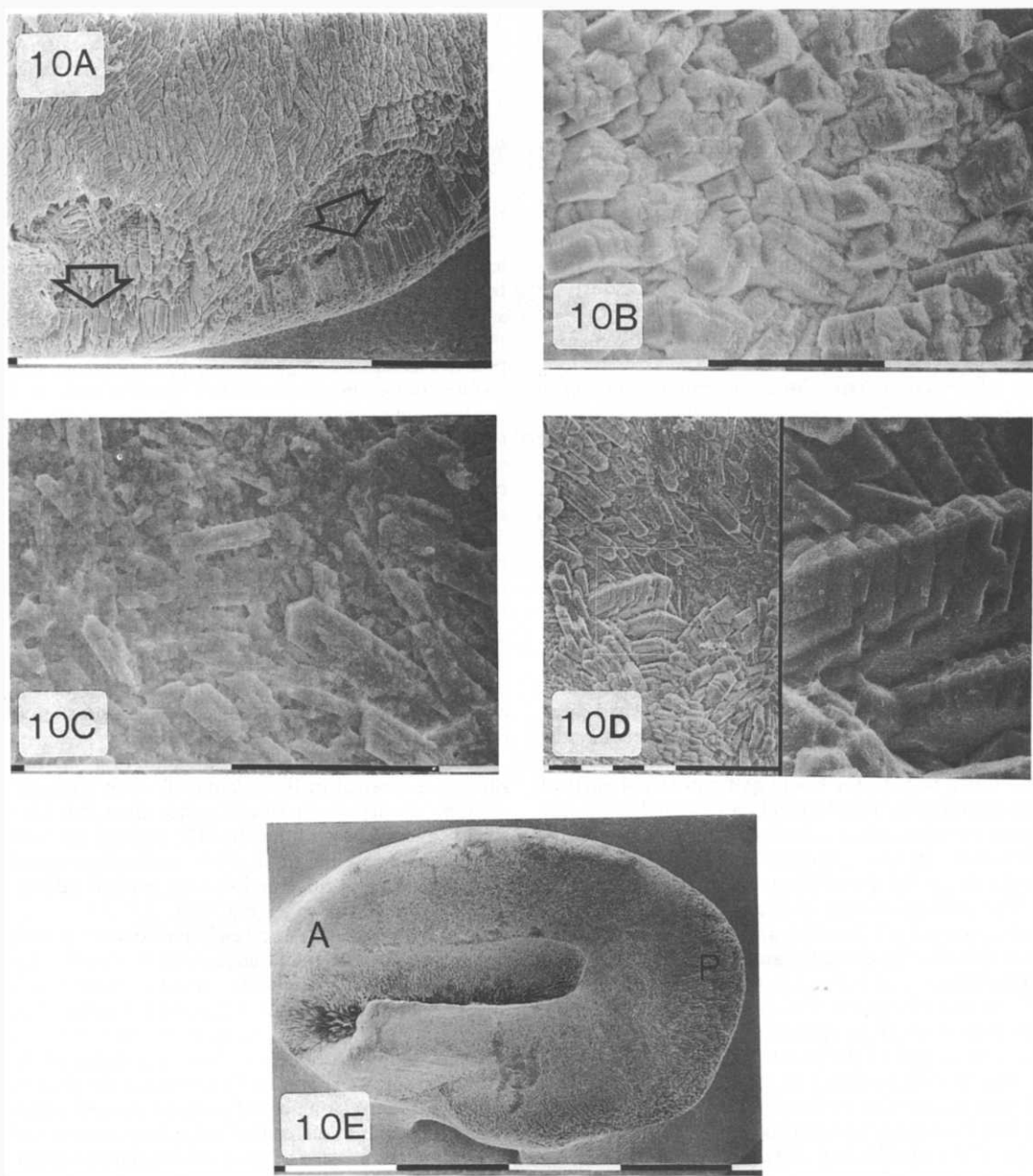


Fig. 10. (A) A damaged part of the anti-sulcus surface showed the large aragonite crystals of the otolith with evidence (arrows) of layering of crystals. The bar is 1 mm. (B) Crystals at the edges of the anti-sulcus surface showed a block-like pavement of crystals. The bar is 0.1 mm. (C) Recrystallisation into a small amorphous crystal cement occurred on some parts of the anti-sulcus surface. The bar is 0.1 mm. (D) Recrystallisation into stacked platelets occurred on parts of the anti-sulcus surface. The bar is 0.1 mm. (E) The sulcus surface of the otolith of *Halosaurus pectoralis* has a deep, but simple shaped sulcus and no other features other than a coarse crystalline structure are both the anterior (A) and posterior (P) ends of the otolith. The bar is 1 mm.

was smooth and composed of a mat of small crystals. The sulcus surface of the otolith of *A. rostrata* was very complex with a series of parallel ridges and grooves, which, without access to the anatomy of the endolymphatic sac, could not be interpreted as to which was sulcus and which were other structures (Fig. 9B). However, the surface of the sulcus side nearest the edge was formed from a mat of needle-like crystals, and the crystalline texture of the major

groove of the sulcus surface was composed of coarse crystals, aggregated into nodules in some parts of the sides of the main sulcus groove. The differences in size between crystals from the sulcus and anti-sulcus surfaces are shown in Table 1.

A polished section of the widest part of the otolith at the anterior end showed a roughly triangle shaped otolith with an opaque (white by reflecting light) core occupying about a third of the cross sectional area of

the otolith (Fig. 9C). Outside of the central opaque zone there were many narrow, closely-spaced opaque zones in the dorso-ventral axis of the otolith (Fig. 9C). There were a few opaque zones on the anti-sulcus side of the otolith (Fig. 9C). Counting the edge of the central opaque zone as 1, there were 15 single opaque zones from the nucleus to the dorsal edge of the otolith.

The sulcus part of the otolith showed an apparent crystalline in-filling pattern suggesting two sulcus grooves (Fig. 9C), with a much less well defined pattern of opaque zones. A broken section of the otolith of *A. rostrata* showed epitaxial growth with a longer twin crystal and a slightly longer anti-sulcus than sulcus radial crystal twin (Fig. 9D). The broken section of *A. rostrata* showed a pattern of hemispherical spalling lines particularly along the dorsal growth axis. (Spalling lines are abrupt changes in crystal size that result in very smooth crystalline surfaces in broken sections of otoliths, Gauldie, 1987). The otolith of *A. rostrata* was unusual in having smooth surfaces as well as sharply angled and curving surfaces (Fig. 9E).

The calcium surface of the section of the otolith of *Antimora rostrata* showed the triangular appearance of the otolith cross-section with a number of grooves corresponding to the complex architecture of the sulcus surface (Fig. 9F). Raising the calcium floor showed the same tilt in the calcium surface from the anti-sulcus to sulcus edge as observed in other otoliths as well as a series of more-or-less parallel ridges running from the sulcus to anti-sulcus surface (Fig. 9G).

The strontium surface of the section of the otolith of *Antimora rostrata* showed much higher strontium counts in the sulcus part of the otolith with a series of peaks equivalent to the sulcus peak found in some other otoliths (Fig. 9H). Ridges of heightened strontium counts run from the anti-sulcus surface to the central dorso-ventral growth axis that has the minimum strontium counts (Fig. 9H). There were about 10 countable ridges in strontium count between the nucleus and the dorsal edge of the otolith.

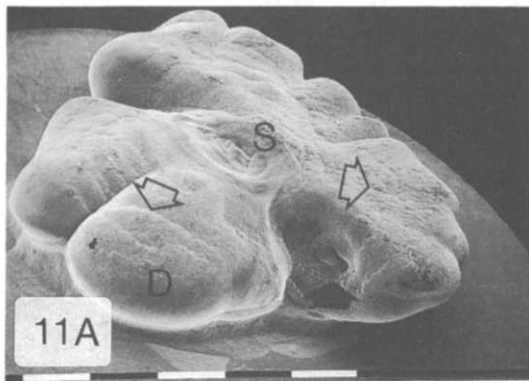


Fig. 11. (A) The sulcus surface of the otolith of *Neophryinchthys angustus* had a bi-lobed dorsal (D) part with a ridged surface (open arrows). The ventral part has a scalloped edge with ridges (open arrows) radiating from the sulcus. The sulcus (S) was small and circular with a ridged interior. Another sulcus-like structure was located on the dorsal edge of the ventral segment (arrow). The bar is 1 mm. (B) Detail of the sulcus-like structure on the ventral part showed a grooved centre and coarsely crystalline surfaces (open arrow). The ridges (arrow) of the ventral part can be clearly seen. The bar is 1 mm.

Halosaurus pectoralis (*Halosauridae*)

Halosaurs are deep water fishes occurring in a number of anatomically similar species. *Halosaurus pectoralis* is found in New Zealand waters and the otoliths used in this study came from a specimen (40 cm TL) taken at 1000 m.

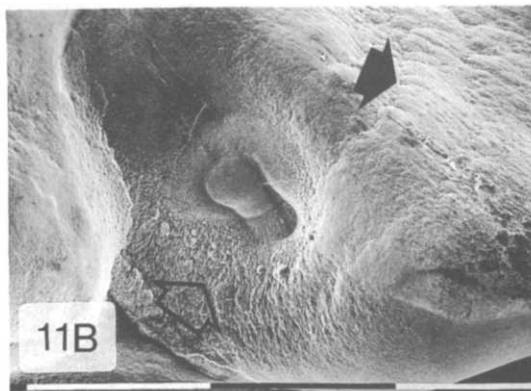
The anti-sulcus surface of the otolith of *H. pectoralis* showed a very coarse crystalline structure both at the edge and more central parts of the otolith giving the anti-sulcus surface a rugose appearance. Part of the anti-sulcus surface of the otolith had been damaged and showed the internal part of the otolith was composed of massive crystals of aragonite, 100 times longer in diameter than any observed on the anti-sulcus surfaces of any other otoliths (Fig. 10A). The edge of the anti-sulcus surface showed a massive block-like pavement of crystals of the same kind (although much larger) than were observed in the sulcus of other otoliths (Fig. 10B), although in some places recrystallisation to both small amorphous crystals (Fig. 10C) and stacked platelets occurred (Fig. 10D). The anti-sulcus surface had a groove running from the centre of the otolith to the dorsal edge. The crystals of the anti-sulcus surface gave the appearance of growing away from the central point of the anti-sulcus surface towards the otolith edge.

The otolith of *H. pectoralis* had a deep sulcus opening at the posterior end, with a coarse crystalline structure over almost the entire anti-sulcus surface (Fig. 10E). The crystal structure of the anti-sulcus surface was most coarse at the edge, becoming progressively less coarse towards the edge of the groove of the sulcus with large lath-like crystals within the sulcus. The differences in size of crystals between the sulcus and anti-sulcus surfaces are shown in Table 1.

Psychrolutes obesus (*Psychrolutidae*)

The deep water sculpin *P. obesus* (26 cm TL) was caught at 1050 m in New Zealand water.

The otolith of *P. obesus* was divided along antero-posterior axis into a longer ventral part with scalloped edges and a bi-lobed dorsal part. The surface



of the anti-sulcus side of the otolith consisted of a pavement of small laths more or less orthogonal to the surface. The sulcus surface was more complex. The bi-lobed dorsal part showed a series of ridges on the surface radiating from a small, round sulcus (Fig. 11A). However, a second sulcus-like structure appeared on the dorsal edge of the ventral part of the otolith, almost at 90° from the first sulcus (Fig. 11A). The second "sulcus" showed a coarse crystalline appearance (Fig. 11B). The ventral part of the sulcus surface was broken into prisms at the edge (Fig. 11A), and also showed a series of ridges radiating from the sulcus (Fig. 11A). More detail of the ridges can be seen in Fig. 11B, but at higher magnification the ridges were formed by changes in the depth of the mat of surface crystals. These crystals showed the 64° twinning angle as an integral part of their organisation. A section broken along one of the dorsal lobes showed an epitaxial crystal organisation with a long medial twin with asymmetric radial twins, the sulcus twin being much shorter than the anti-sulcus twin. The differences in size of crystals between the sulcus and anti-sulcus surfaces are shown in Table 1.

Neophryinchthys angustus (Psychrolutidae)

The pale toadfish is a rather repulsive toadlike fish with the appearance and consistency of jelly. The sculpin has very large head and is evidently a sedentary fish similar in appearance to *Psychrolutes obesus* and probably similar life habits. The specimen

(28 cm TL) from which the otoliths were taken was caught at 800 m in New Zealand waters.

The anti-sulcus surface of the otolith of *N. angustus* showed a division into a dorsal and ventral half with a number of prisms on the dorsal half. The surface of the anti-sulcus side was composed of a mat of crystals. On some part of the surface the crystal mat was organised around the 64° twinning angle, with indications of possible dissolution and recrystallisation towards the centre of the otolith. The edges of the otolith were marked by a narrow groove, towards which the surface crystals at the edge become progressively more oriented. The sulcus surface of the otolith of *N. angustus* showed a shallow sulcus with two major and asymmetrical components. The crystalline surface of the sulcus side of the otolith had a similar mat-like appearance to the anti-sulcus side becoming progressively more organised into what appeared to be weakly defined prisms within the sulcus half. A broken section of the otolith showed epitaxial growth with a long-radial twin along the dorso-ventral axis with a shorter and longer medial twin towards the sulcus and anti-sulcus surfaces respectively. The differences in size of crystals between sulcus and anti-sulcus surfaces are shown in Table 1.

Fossil otoliths

Broken sections of the otoliths of fossil species typically showed a crystalline interior composed of

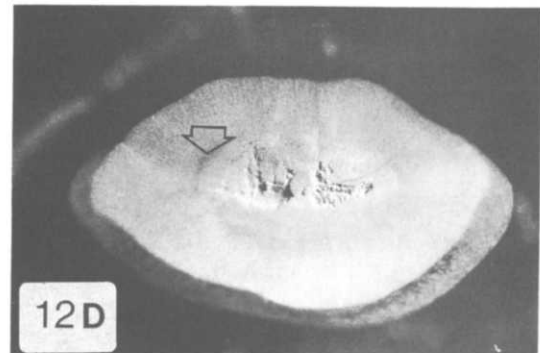
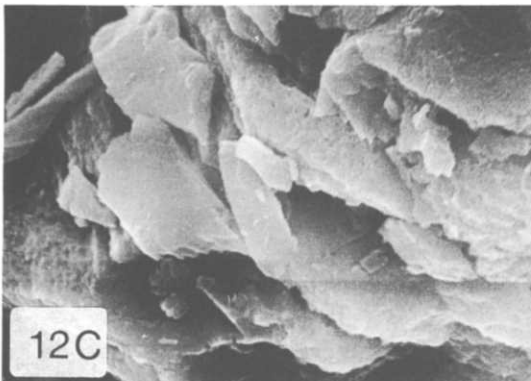
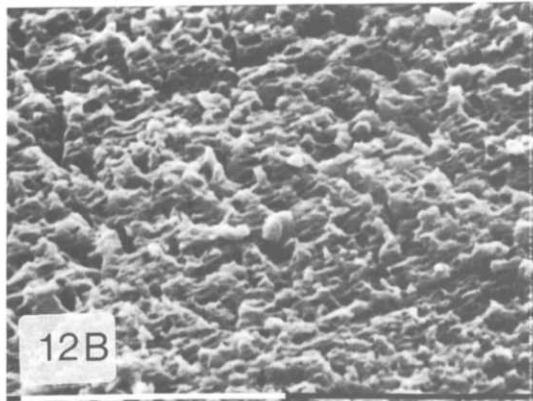
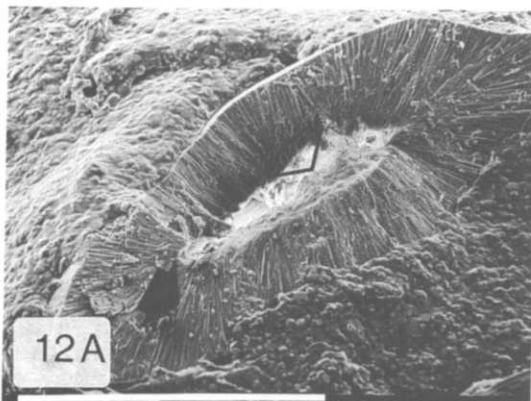


Fig. 12 (A)-(D). *Caption on opposite page*

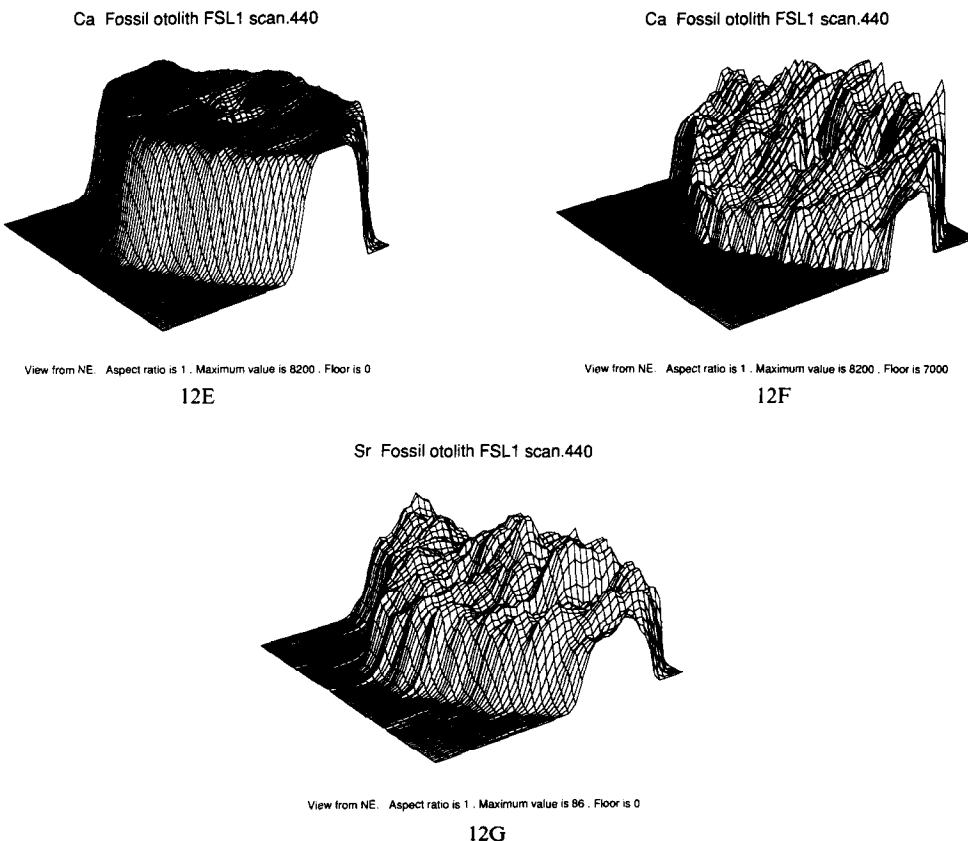


Fig. 12 (A) Broken sections of a fossil otolith showed a markedly crystalline interior composed of large crystals arrows (arrows) with recrystallisation at the centre of the otolith into an amorphous crystalline mass (open arrows). The bar is 1 mm. (B) The external surfaces of the fossil otolith were smooth, consisting of very small crystals. The bar is 10 μm . (C) The centre of the otolith was composed of a mass of large crystals, with few morphological characteristics. The bar is 10 μm . (D) A fossil otolith was sectioned along the dorso-ventral axis and polished showing the re-crystallised centre and the strongly radiating crystal pattern. Opaque zones appeared on the section surface (arrow) but were weakly defined. (E) The calcium surface of the otolith showed a central pit corresponding to the area of recrystallisation and weakly defined ridges running parallel from the anti-sulcus to sulcus edge. (F) Raising the floor of the calcium surface emphasizes both the tilt and the sulcus to anti-sulcus ridges. (G) The strontium surface of the fossil otolith showed a peak in strontium counts corresponding to the pit of recrystallised materials as well as weakly defined ridges running from the anti-sulcus to sulcus edge.

large crystals (Fig. 12A) with smooth external surfaces (Fig. 12B) and indications of recrystallisation in the central part of the otolith (Fig. 12C).

A fossil otolith with a well-preserved external appearance was sectioned horizontally along the dorso-ventral axis (Fig. 12D). This section was polished and showed by reflected light that the central part of the otolith had been dissolved and apparently recrystallised. Light and dark zones were present in some of the rest of the otolith but it was not possible to determine from their appearance if they were equivalent to opaque and hyaline zones.

The calcium surface of the fossil otolith showed weakly defined ridges running more-or-less in parallel from the anti-sulcus to sulcus surface, but with a central pit corresponding to the area of recrystallisation observed in the light microscope (Fig. 12E). Raising the calcium floor further emphasizes the tilt from anti-sulcus to sulcus surface, which is, like *A. rostrata* higher at the sulcus surface (Fig. 12F).

Raising the calcium floor also showed the sulcus/anti-sulcus ridges more clearly as well as the pit in calcium content in the central of the otolith (Fig. 12F).

The strontium surface of the sectioned otolith showed less well-defined ridges running from the sulcus to anti-sulcus surface (Fig. 12G). There was a pronounced increase in strontium counts in the part of the otolith corresponding to the pitted, recrystallised central part of the otolith (Fig. 12G).

Crystal sizes were measured directly from photographs to give average crystal size at the anti-sulcus and sulcus surfaces (Table 1), and depth of capture. Crystal sizes for anti-sulcus and sulcus are plotted against depth of capture in Fig. 13.

DISCUSSION

The otolith of the sample of deep water fishes described in this paper showed a number of similar features. With the exception of *Antimora rostrata*, the

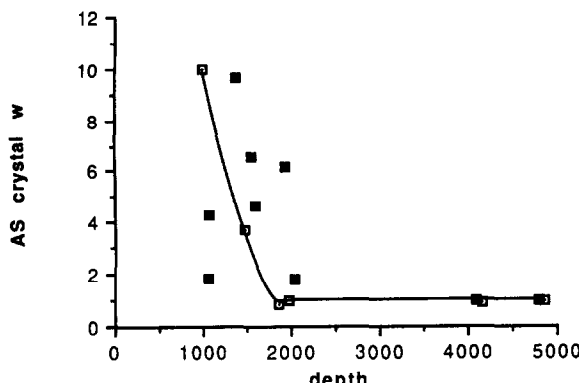


Fig. 13. The widths of anti-sulcus crystals (□) and sulcus crystals (■) are plotted against depth of capture. The general line for crystal size variation by depth was fitted by eye.

otoliths tended to have a rounded, flattened appearance with a poorly developed prismatic structure. The otolith of *A. rostrata* had the most complex shape with what may have been a multi-lobed macula. The otoliths of *Psychrolutes obesus* and *Neophrynidichthys angustus* also showed indications of either more than one macula lobe, or even two separate maculae associated with the same otolith. The shape of the otolith of teleosts is generally related to the spectrum of sound frequencies to which the fish inner ear is most sensitive (Gauldie, 1988b). The ratio of sulcus area to otolith area for the otoliths in this study (Table 1) ranged from 0.03 to 0.28 (ignoring multi-sulcus effects). Following Gauldie (1988b) these values suggest that most of the otoliths of these fish have sensitivities at low frequencies, i.e. effectively 'listening', in the far field. Most of the fish examined in this study have large eyes, sensory pits and barbels as well as elaborate lateral line systems on an elongate body form suggesting that they need not rely on the auditory mechanisms of the inner ear to explore the near field and consequently their otolith have become adapted to sensitivities in the low frequency range enabling them to act as potential detectors of large body movement in the far field. The lowest value, 0.03, was recorded for *Psychrolutes obesus* whose common name, blobfish, clearly indicates its slow-moving, the bottom-living habits. The lowest values of the macula/otolith ratio reported by Gauldie (1988b) were for bottom dwelling fishes.

Sections of the otoliths showed a consistent feature of deep water otoliths, the continuity of opaque zones from the sulcus part of the otolith, through the central growth axis to the anti-sulcus part of the otolith. In the otoliths from more shoal species those opaque bands stop when they reach dorsal and ventral (*in situ*) margins of the otolith (e.g. Gauldie, 1987). This behaviour has been used in part to explain the use of check rings in ageing fish (Beamish, 1979) i.e. growth continuing on the sulcus face of the otolith and not on the anti-sulcus face. The continuity of the opaque zones implies a mineral deposition environment right around the otolith. The lack of a marked sulcus groove in many of the otoliths examined in this study also suggest a more uniform deposition of crystal.

The exception to these observations was the halosaur otolith, which has a very deep, well defined sulcus. However, the halosaur also has the largest crystals that we have so far observed in any otolith calcium carbonate. Such large crystal size implies very slow growing crystals which in turn implies a more acidic crystallisation environment; given that calcium ion concentration must be maintained within certain concentration limits if the inner ear is to function at all. The crystallisation evident in the cementation observed in halosaur otoliths also implies an environment close to the equilibrium point of dissolution and recrystallisation.

Broken sections of otoliths showed crystalline features common to all teleost otoliths. All broken sections had the appearance of aragonite crystals with medial and radial twins growing from a central nucleus. Crystal size within the otolith varied between species ranging from very large in *Halosaurus pectoralis* to size more typical of teleosts in the macrourids. In addition, direct observations of growing crystals on the surface of the otolith showed a consistent pattern of crystals, intersecting at 64°, the aragonite twinning angle (Gauldie and Nelson, 1988), indicating that the fish overcome the depth-related change in stability of aragonite towards calcite.

Crystal size on the exterior surfaces of the otolith varied by almost an order of magnitude between species. In most cases the crystals of the sulcus were larger than the crystals of the anti-sulcus surface except in *Halosaurus pectoralis* in whose otolith the crystals of the sulcus were smaller than those of the anti-sulcus surface. However, both sulcus and anti-sulcus surface crystals of the otoliths of *Halosaurus pectoralis* were much larger than those found in other otoliths. Plotting crystal size by depth of capture showed that above 2000 m crystal size was variable ranging from small to large, but below 2000 m crystal sizes were small. Crystal size is a reflection of crystal growth rate. If pH is a major determinant of otolith crystal growth rate as suggested by Gauldie and Nelson (1990a), then one could interpret small crystals that indicate rapid growth as an indicator of increasing alkalinity in the endolymphatic fluids with increasing depth.

Sections of otoliths showed that the nucleus of the otolith was most often situated closer to the sulcus than to the anti-sulcus side of the otolith. The sulcus itself was often filled-in with crystalline material leading to a shallow sulcus. The otoliths of *Halosaurus pectoralis* were exceptional in that they had a very deep sulcus in comparison with the other otolith examined. With the exception of *H. pectoralis* the otolith showed deposition patterns that were more uniform around the otolith without either the very slow deposition rates typical of the sulcus in other fishes, or the slow deposition rates typical of the anti-sulcus surface in other otoliths. These observations also point to a uniformly alkaline environment with slight gradients in pH in the fluids of the endolymphatic sac between the macula and the point of crystallisation. The metabolic rate of *Coryphaenoides armatus* is very low (Smith, 1978) about one-tenth of that of the cod (Saunders, 1963). The macrourids generally showed decreasing size and uniform growth around the otolith which would be

consistent with high pH maintained by low metabolic rates. The unavoidable implication is the *Halosaurus pectoralis* has a fundamentally different metabolism to that of the macrourids. Depth-related crystalline effects suggest that other aspects of the chemistry of the otolith may also be depth-affected.

The chemistry of the otoliths showed a number of consistent features. Calcium surfaces were almost always tilted from the anti-sulcus (high) to sulcus (low) edges of the otolith. Calcium surfaces showed a series of weakly defined more-or-less parallel lines running from the sulcus to anti-sulcus side in almost every otolith examined.

Strontrium surfaces typically showed a more complex behaviour than their corresponding calcium surfaces. Strontium levels in the filled-in part of the sulcus (i.e. the apex of the sulcus below the nucleus) were typically higher than in the rest of the otolith. Many otoliths showed a ridge of increased strontium counts along the dorso-ventral axis of the otolith separated by a shallow groove from heightened strontium counts at the edges of the otolith.

The similarities and dissimilarities in the pattern of crystalline structure and chemistry of the otolith present an opportunity to relate the chemical codes of the otolith to the life history of individual fish. The individual life histories of deep water fishes are hardly understood at all, but there are certain clues offered in the depth range of species that show the deep ocean to be stratified vertically in a way that ought to reflect life history strategies.

All demersal species occupy discrete sounding ranges (e.g. see Haedrich and Merrett, 1988); some occur within relatively narrow strata (e.g. *Hoplostethus atlanticus*—Gauldie *et al.*, 1989), while others occupy broad ranges (e.g. *Synaphobranchus kaupi*—Haedrich and Merrett, 1988). Within their sounding ranges some species follow a 'smaller-shallower' trend, while others do not (see Merrett *et al.*, in press a). Species richness is greatest on the slope; in the North Atlantic Basin 77% of species are unique to the slope, 23% to the rise and 34% to the abyss (Haedrich and Merrett, 1988). Specifically, in the Porcupine Seabight area of the eastern North Atlantic where the majority of the currently reported samples came from, some 133 species were encountered between 247–4787 m soundings, of which the ranges of only 13 commenced below 2200 m soundings and only a further 30 extended beyond this level from higher on the slope (Merrett *et al.*, in press, a,b).

Information gathered from sampling has often been restricted to size frequency distribution by depth, which may change by season and over the geographical range of the species. Some of the variation in size frequency can be matched to oceanographic data and secondary data such as gut content to give some clues to the history strategies of different species that lead to their characteristic distribution in the water column. However, such data are patchy and very likely to be a statistical under-sample giving us only 'windows into a sea of confusion' (Angel, 1977).

An alternative approach would be to use the life history data stored in the chemical composition, particularly in the strontium of fish otoliths. However, increasing knowledge of the intra-specific and

inter-specific variation in otolith chemistry (Gauldie *et al.*, 1986; Townsend *et al.*, 1989) has only served to reinforce the need to develop a proper theoretical basis for the observed variation in otolith chemistry. A need that was first expressed by Odum (1957) in his 'Circulation Theory' of the elemental composition of biogenic calcium carbonates. In our current state of knowledge we are still a long way from a complete theory, but there are three useful approaches that can be applied to the problem. These are physiological, chemical and crystallographic and are developed separately in the following sections.

Physiological perspectives

Odum (1957) showed that the strontium uptake into biogenic calcium carbonate minerals (including otoliths) had a distribution factor indicating that the variation in the degree of exclusion of strontium from the mineral among different species was a taxonomic property. This interspecific variation was unrelated to the low levels of strontium:calcium ratios in freshwater compared to saltwater fishes (which is about 1:4), since the lower levels of strontium in freshwater lead to uptake ratios similar to those in saltwater (-3.4 in fresh, cf. -2.3 to -3.0 in salt). A 'taxonomic property' is of necessity a genetic and therefore physiologically determined property. This view is reflected in the argument of Lowenstam (1964) that strontium to calcium ratios decrease in phylogenetically advanced organisms, being preferentially excluded by more complex calcification processes. (However, as a group, molluscs appear to be unique in their ability to selectively discriminate against strontium (Likins *et al.*, 1963), with a tendency towards increasing strontium content with greater physiological complexity within at least the calcite-using group of organisms (Milliman, 1974)).

Freshwater teleosts typically have lower skeletal strontium to calcium ratios than those of saltwater teleosts, (ranging from 0.11×10^{-3} to 0.42×10^{-3} for freshwater fish, and from 1.35×10^{-3} to 3.90×10^{-3} for saltwater fish (Odum, 1957)). In a study of the strontium content of bones in different fish species from a high strontium content, and a low strontium content lake (strontium went from 0.03 to 0.034 in the low lake, to 0.1 to 0.12 in the high lake and the Sr/Ca ratio was 1.89 in the high Sr lake and 2.33 in the low Sr lake), there was a significant difference between lakes in only one of the five fish species sampled, and overall, four species had similar Sr/Ca values (0.19×10^{-3} to 0.24×10^{-3}) compared to 0.66×10^{-3} for the fifth species (Ophel and Judd, 1967). The strontium content of the otoliths of fishes is generally lower than the strontium content of statocysta and statoliths from molluscs (Lowenstam *et al.*, 1984). The otoliths of fishes typically show strontium to calcium ratios from 0.67×10^{-3} in freshwater to 3.9×10^{-3} in marine fishes (Odum, 1957).

The strontium content of mollusc shell increases in some species with temperature, but decreases with others (Pilkey and Goodell, 1963; Dodd, 1965; Lehr, 1965; Hallam and Price, 1968). Strontium levels in the test of the echinoderm *Dendraster excentricus* was found to be inversely related to temperature and is unaffected by salinity (Pilkey and Hower, 1960). Strontium levels in fish otoliths decrease with

temperature in most fishes in a species-specific way (Townsend *et al.*, 1989; Radtke, *et al.* 1989), and there is circumstantial evidence for sex, size and location dependent variation in strontium to calcium ratios in sockeye salmon from two different lakes that are known to have different temperature regimes (Gauldie *et al.*, 1980). The general physiological responses of organisms that could cause fluctuations in the strontium to calcium ratios of mineralized tissues appear to be complex without any single factor that can be singled out that might point to a specific physiological mechanism.

However, ionic regulation in teleosts is strongly affected by ATP-ase activities in the gills which is often dependent on the ratio of calcium to magnesium. Thus, in a crude sense, there may be ATP-ases in fish gills that have been selected for by high and low Ca/Mg environments—which, given the intimacy of gills and their environment, may be directly sensitive to ambient ion content. If this kind of active uptake was the mechanism of strontium variation then this temperature dependency could be inferred from the Teorell–Ussing equation (Netter, 1969) that describes equilibria of ion concentrations across membrane. The Teorell–Ussing equation contains a term, $\exp. (I/T)$, where T is the Kelvin temperature. Although this term indicates an inverse relationship with temperature, the implied rate of change with temperature is far below what has been observed indicating active membrane uptake to be at best a minor component of the strontium variation. A further consequence of this argument would be that strontium levels in the water do not affect strontium uptake over the normal physiological range of tolerance of the fish.

However, the evidence points to a physiological mechanism that underlies the variation in the strontium and calcium uptake of mineralised tissues that is species, rather than environment, specific; and possibly class specific as well (Rosenthal, 1981). Strontium can replace calcium in divalent ion permeability changes in membranes, and in many ion transport situations strontium is biochemically similar to calcium (Porzig, 1981). However, strontium replacement of calcium past a certain level is physiologically deleterious which probably underlies the species-specificity of strontium distribution in hard parts (Johnson *et al.*, 1968) as well as indicating a non-linearity in uptake against ambient concentrations. One of the general effects of membrane transport is to protect the organism from loading its plasma with concentrations of ions deleterious to the physiology of the organisms. Unfortunately the inevitable non-linearity of plasma ions against ambient (or dietary) ions is often lost from sight in the statistical assumptions made in many studies aimed at geographic population separation which assume that the ion concentrations of the hard parts of fishes are linearly related to those in their environment. The effect of the discrimination against strontium is to produce two pools of strontium. An initial labile pool in which there is no physiological discrimination between strontium and calcium, and a secondary, less labile pool of lower strontium to calcium ratio, reflecting the maturation of the mineral phase (Lengemann, 1960; Neuman *et al.*, 1963; Storey

and West, 1971). A consequence of this two-pool system would be that plasma strontium to calcium ratios would exceed those of bone, and this situation has been observed (Kshirsager *et al.*, 1966). Under these circumstances mobilisation of calcium from the mineralised tissues during periods of rapid crystallisation at higher temperatures could result in a decrease in the stontium to calcium ratio as the influx from the less labile, distal pool of calcium dilutes the strontium content of the more labile, proximal plasma pool. However, the implied gradients in discrimination against Sr are small and, as with membrane transport, could only be, at best, a minor component of the temperature dependence of strontium uptake.

Chemical perspectives

Once in the fluids of the endolymphatic sac, the fate of all ions that are incorporated into the growing otolith crystal are affected by the chemistry of precipitation. Assuming that no new crystals form during otolith growth, then the rate of change of ion concentration in solution that is equivalent to the rate of growth of the crystal surface is given by:

$$-\frac{dI}{dt} = k \cdot S^\circ \cdot ((AP)_i^{1/2} - (K_{sp})^{1/2})^n$$

where k is the rate constant, S° is the free surface area available for growth, $(AP)_i$ is the concentration product of the ion at time t , (K_{sp}) concentration solubility product, and n is the effective order of reaction. The term S° is a function of the total crystal surface area S , and in the presence of inhibitors, or any other effective control of the surface area available to ion absorption, the competition (or binding at the crystal surface) is defined by the Langmuir adsorption isotherm,

$$S^\circ = S/(1 + b(IN)),$$

where b is a constant and (IN) is the concentration of free inhibitor in solution.

Substituting the adsorption term into the general equation, and considering calcium precipitation, yields,

$$-\frac{dCa}{dt} = \frac{k \cdot S \cdot ((AP)_i^{1/2} - K_{sp})^{1/2})^n}{1 + b(IN)}$$

where the effective order of reaction for calcium carbonate is 2. The effect of this complex of factors is that crystals only stop growing when $S = 0$, when $(AP)_i = K_{sp}$, or when the (IN) term is very large, resulting in equilibrium occurring only under unusual conditions so that the approach to equilibrium will be slow, if convergence occurs at all. One effect of this system is that at the point where it is slowly approaching equilibrium, it will favour the slow growth of large crystals.

In general terms, the expression for ion concentration decay depends on the surface of crystal, the amount of cation and anion, factors that control the solubility of the cation and anion and any inhibitors (or even accelerators) of crystallisation. In particular, the relation between $(AP)_i$ and K_{sp} means that either concentration or solubility product (e.g. pH dependent solubility) can exert simultaneous or independent control over precipitation rate. The expression for calcium also applied to the other ions, including

strontium and zinc that are precipitated into the otolith crystal.

The concentration term of calcium can be expected to be controlled within physiological limits since the ambient calcium ion concentration affects the depolarisation characteristic of the neuropile of the macula that is bathed in the endolymphatic fluid (Hubbard *et al.*, 1969). Seasonal variation in free calcium ions has been reported to range from a low of 65.4% of total calcium levels during fast growth, to a maximum of 79.1% during slow growth (Mugiya, 1966). This is probably the maximum physiological range over which Ca^{2+} ions can vary without nervous dysfunction. It is evident from these considerations that the rate of calcium ion concentration decay requires control, if not direct inhibition, to ensure that adverse depolarisation effects are not caused by excessive lowering of levels of free calcium ions.

The effect of these restrictions is to make the concentration product term (AP), more-or-less constant. If it is assumed that the surface area of the otolith is so large as to be constant, then only the amount of inhibitor (IN) and the concentration solubility product K_{sp} are left as potential modulators of otolith growth. In the model of Gauldie and Nelson (1990a) both mobilisation of calcium and subsequent recrystallisation on to the otolith are controlled by the same mechanism, metabolically driven pH gradients that change the local solubility product term K_{sp} along the sulcus face of the otolith. In addition to metabolic effects, temperature also affects pH in the blood, and presumably other bicarbonate buffered fluids, so that pH decreases as temperature increases leading to a general relationship $\Delta\text{pH}/\Delta T = -0.016$ (Howell *et al.*, 1970). A decrease in temperature of 10°C would lead to an increase in pH of 0.16 pH units. Changes in pH of this order would result in an increase in the deposition rate of the otolith. Even without pH effects, studies of strontium carbonate solubility products in aqueous solutions show a decrease of about 32% between 25 and 50°C (Sonderegger *et al.*, 1976). It can be seen from the general equation that a decrease in K_{sp} leads to an increase in the rate of precipitation of the ion from solution if all other conditions including pH are constant. This effect alone would account for about a 13% increase in strontium with temperature over the normal 10°C physiological range.

The inhibition term (IN) is usually taken to refer to organic material, the protein and other organic material that forms the matrix of most biogenic carbonates. However, as Morse and Mackenzie (1990; p 81) point out, "when all else fails to explain carbonate kinetic behavior, organic matter is usually given the credit". This has been the case in the otolith studies of Kalish (1989), although an unrecognized mixture of different species in the sample and handling stress were more likely to have been involved. Otolith organic composition decreases as the otolith increases in size (Morales-Nin, 1986; Gauldie *et al.*, 1990). Nonetheless, calcium carbonate precipitation is inhibited by organic matter (Berner *et al.*, 1978). Molluscan aragonites have many similarities to otolith aragonite and the periodic check-ring-like structures that imply temporary slow-

ing, or even cessation, of growth in molluscan aragonites are associated with an ordered deposition of polysaccharides and proteins (Weiner and Traub, 1984). By definition, such organic interstices imply inhibition of crystal growth. Analysis of the relative patterns of the organic deposition associated with daily microincrements and the patterns of crystal deposition in a number of otoliths showed that the patterns, at least, of organic and crystal material were not correlated (Gauldie and Nelson, 1990b). The implication is that although the organic component may sequester strontium ions it may be doing so independently of the strontium ion uptake of the crystal phase. The organic matrix of non-carbonate calcified tissue has been shown to sequester strontium ions even to the extent of displacing up to 6% of the calcium off the matrix by heterionic exchange (Jethi *et al.*, 1972).

In addition, artificial aragonitic ooids grown on a simple humic acid matrix showed very high strontium to calcium ratios ($5.9-8.4 \times 10^{-2}$ weight ratio) that were unrelated to the magnesium content of the ooid (Suess and Fütterer, 1972) and, for want of a better explanation, might be associated with the unusual organic component of ooids. To some extent the effect of the organic matrix on the crystallisation process can be gauged from the co-existence of large and small otoconia in the endolymphatic sac of elasmobranchs (Mulligan and Gauldie, 1989), chimaeras (Gauldie *et al.*, 1987; Mulligan *et al.*, 1990) and the Australian lungfish (Gauldie *et al.*, 1986). Under normal conditions of crystallisation, the process of Ostwald crystal ripening would lead to the dissolution of smaller otoconia in favour of the larger crystals. That this doesn't happen is evident from examination of the otoconial mass in elasmobranchs and chimaeras which shows that under biological conditions in the endolymph, crystallisation is maintained far away from equilibrium conditions presumably by the inhibition effect of the protein matrix. In addition to the effects of the solubility product and organic component on the strontium content of otoliths, there are crystallographic effects on the strontium/temperature relationship.

Crystallographic perspectives

Direct measures of the distribution coefficient of strontium in artificially precipitated aragonites showed a decrease in distribution coefficient with temperature of about 30% from 16 to 96°C (Kinsman and Holland, 1969). The distribution coefficient is defined as:

$$\frac{M_{\text{Sr}^{2+}}^A}{M_{\text{Ca}^{2+}}^A} = \frac{K_A^A \cdot M_{\text{Sr}^{2+}}^L}{\text{Sr} M_{\text{Ca}^{2+}}^L},$$

where the ratio ($M_{\text{Sr}^{2+}}^A/M_{\text{Ca}^{2+}}^A$) within the aragonite is related to the ratio ($M_{\text{Sr}^{2+}}^L/M_{\text{Ca}^{2+}}^L$) in solution by the distribution coefficient K_A^A . Over the normal physiological range of about 10° , the distribution coefficient predicts about a 4% increase in strontium.

Swan (1957) pointed out that the variation in strontium to calcium ratios in mollusc shell was related to shell thickness, which was in turn related to growth rate; slower growing molluscs having

thicker shells. The question of the effect of growth rate (or more correctly, precipitation rate) was taken up by Lorens (1981) who observed an anomalous behaviour in strontium ion incorporation into calcite, in which, (unlike other metal ions), there was an increase in the strontium distribution coefficient with increasing precipitation rate of the calcite crystal. Lorens offers the following explanation:

"Strontium, with a crystal ionic radius 28% larger than that of Ca^{2+} , prefers the more open, octahedral, crystal structure of aragonite to the hexagonal structure of pure SrCO_3 . When initially adsorbed, steric constraints are minimal since Sr^{2+} is coordinated with relatively few carbonate oxygens; this may allow a higher D than is allowed for a fully coordinated Sr in the calcite lattice. With increasing precipitation rate, less time is available for equilibrium at each degree of coordination and the observed D increases with precipitation rate as more of the high D Sr is trapped in the crystal lattice."

Crystals grow large at lower temperatures, but more slowly. If Lorens' argument is correct, one would expect strontium levels to decrease with temperature, which is what we observe. Lorens went further by showing that the distribution coefficient for strontium observed in *Mytilus edulis* was consistent with bulk estimates of crystallisation rate in the shells of the mollusc. Lorens' results agree with the earlier results of Katz *et al.* (1972). However, a later study by Mucci and Morse (1983) provided directly contradictory data. Mucci and Morse showed that strontium incorporation into calcitic overgrowths was not related to precipitation rate, but was linearly related to the magnesium content of the calcite.

The difference between the results of Lorens (1981) and Mucci and Morse (1983) may have been due to a difference in approximate equilibrium conditions, leading to the development of two different kinds of distribution coefficients, one based on heterogeneous conditions (the Doerner-Hoskins relation used by Lorens), the other on homogeneous conditions (the Henderson-Kracek relation used by Mucci and Morse). In effect, Lorens treatment examines the effects of precipitation rate in term of the initial and final states of both the metal and calcium ions both in the crystal and in the solution. On the other hand, Mucci and Morse stabilised conditions so that precipitation rate did not change the initial and final conditions. Changes in precipitation rate of the otolith have been shown by Mugiya (1966) to affect initial conditions, therefore the results of Lorens may be more appropriate for comparison with otoliths. Nonetheless, some molluscs (mostly with calcitic shells) show an increase in strontium with increasing temperature.

The aragonite-strontianite problem was examined by Plummer and Busenberg (1987) from the point of view of the chemical behaviour of what is in effect a solid solution of strontianite in aragonite within the otolith crystal. Recrystallisation experiments by Plummer and Busenberg (1987) showed that there was a broadening of X-ray reflections from certain lattices accompanying a shift in D -spacing to more strontium rich compositions, reflecting the conclusions of Lorens (1981). In addition, Plummer and Busenberg showed that activity, and activity co-

efficients of SrCO_3 reflected the partial concentrations of SrCO_3 in CaCO_3 as would be expected from Henry's Law. At low concentration of SrCO_3 in CaCO_3 in $\text{SrCO}_3/\text{CaCO}_3$ solid state solution the activity at 76°C is about 26% of the activity at 25°C. Activity coefficients at the same molefraction of SrCO_3 (by extrapolation) have about half the value at 76°C that they do at 25°C. In the general expression for rate change of an ion a decrease in activity coefficient causes a decrease in precipitation rate. The amount of strontium found in otoliths is about 0.13% by weight (Gauldie *et al.*, 1986) which is about 0.22 molefraction of SrCO_3 and would put otolith strontium into the range of partial solutions that result in a large decrease with temperature. If the values of Plummer and Busenberg (1987) are linear, then SrCO_3 values drop about 1% of the value at 25°C for every degree rise in temperature. However, Plummer and Busenberg point out that the Sr/Ca ration in marine aragonites is about 10 times higher than the Sr/Ca ratio in water. Comparison of inorganic aragonites and biogenic aragonites indicated that there were kinetic processes in biological systems as well as in inorganic aragonites, responsible for the disequilibrium gradient (Plummer and Busenberg, 1987). Observations of intra-specific variation in otolith Sr levels also suggest that there is some kind of biological effect (Townsend *et al.*, 1989). The values quoted for Sr change with temperature by Radtke *et al.* (1989) indicate a change of about 3% per degree. Given the assumption of linearity, and the biological effect, this value can be regarded as consistent with the results of Plummer and Busenberg (1987).

It should be noted that aragonites and strontianites are also effectively solid state solutions with cerussite (lead carbonate) and witherite (barium carbonate) (Speer, 1983) and probably radium carbonate (which is the next higher element to barium in the periodic table). The solid-state solution thermodynamics of the strontium-calcium carbonate series are no doubt implicated in the solid-state solutions of lead, barium and radium carbonates. The problems in using lead and radium series isotope disequilibria in ageing *Macroronus novaezelandiae* described by Fenton *et al.* (1990) could be accounted for more readily by the temperature change in going from juvenile to adult habitat, than by changes in ambient $^{210}\text{Pb}/^{226}\text{Ra}$ concentration ratios. Unfortunately the problems raised by temperature and other kinetic effects on techniques of using radionuclides with fish or mollusc ageing have not been addressed. It is worth noting that Morse and MacKenzie (1990; p. 209) go to the trouble of underlining their statement to the effect that magnesium coprecipitation in marine calcium carbonates is mostly controlled by temperature; and elsewhere they consistently present data to support the general concept that coprecipitation of ions in marine carbonates are strongly controlled by kinetic processes, and are often highly non-linear against ambient concentrations.

Displacement of otolith crystallisation away from equilibrium conditions is further indicated by the anti-pressure effects evident in deep water otoliths. Aragonite solubility increases with depth, rising sharply between 200 and 300 m from negligible levels

to about 2% dissolution per day (based on the shell of *Carolinia tridentata*), and rising slowly from 300 to 3000 m to a maximum of about 4% per day (Acker *et al.*, 1987). This effect is due to the increasing solubility of carbon dioxide under pressure and at low temperatures. Continuing deposition of calcium carbonate by fish otoliths at depths below 300 m requires them to retain alkalinity in the bicarbonate buffered endolymphatic sac against the combined acidifying effect of cold and pressure.

When all three perspectives, physiological, chemical and crystallographic are combined, it is evident that there are probably a number of processes at work that simultaneously cause both an increase and a decrease in the strontium content of the otolith with increasing temperature. The largest single factor appears to be the temperature dependence of activity coefficients of low molefractions of SrCO_3 in $\text{SrCO}_3/\text{CaCO}_3$ solid solutions. The combined effects of membrane effects and organic matrix effects, could be best, only account for 15–20% of the observed variation in strontium. However, given the plasticity of the biology of organisms it is possible that in some species, under some circumstances, what are otherwise minor controls over Sr precipitation may play a major role in determining otolith Sr levels.

In the principal effect of temperature on strontium is via precipitation rate (because activity coefficients refer to the crystal phase), then it is evident that physiological effects that cause changes in precipitation rate other than in response to temperature must be taken into account when using the chemistry of the otolith to recover the life history of the fish. Metabolic stanzas in the life of the fish leave ultrastructural marks in the otolith (Gauldie and Radtke, 1990) possibly because of pH gradient effects (Gauldie and Nelson, 1990). Gradients in pH would lead to episodes of both very fast and very slow precipitation rates, which could be expected to change strontium levels. Such changes would be associated with small and large crystals in the otolith. Therefore translation of strontium levels in the otolith into temperature life history requires corrections to be made for crystal size variation as a proxy for precipitation rate where it can be reasonably inferred from the otolith anatomy that a non-temperature precipitation event may have occurred.

The response of zinc in carbonates to temperature is also complex. Partition coefficients of zinc precipitated with calcium carbonate show a decrease in partition coefficients over temperatures of 25, 35 and 50°C. In addition, recrystallisation may occur causing a shift from homogeneous to heterogeneous conditions (Crocket and Winchester, 1966). However actual levels of zinc observed in mollusc shell (and otoliths) are extremely low compared to tissue (about 12,000 times lower) and could be easily accounted for by the organic fraction of the otolith. A slight increase in zinc content with temperature has been reported for otoliths of chinook salmon by Gauldie *et al.* (1986).

A consistent feature of all of the effects that control strontium in the otolith is that they refer to either physiological or crystallographic control of the distribution coefficient of strontium. Otolith strontium levels are a long way from equilibrium with ambient

seawater, a disequilibrium that is maintained by the physiology and chemistry of the growth processes of the otolith itself.

Interpretation of life histories

Against this background, the interpretation of life histories contained in the chemical composition of the individual otoliths from deep water fishes can be assayed. The strontium surface of the otolith section of *Coryphaenoides armatus* has a pronounced peak in the part of the otolith corresponding to the filled-in sulcus. Since the sulcus is the slowest growing part of the otolith (by definition), its high strontium content may be considered physiological rather than environmental. The nucleus area is a depression in the strontium surface. Following a line from the nucleus along the dorso-ventral axis there are a series of peaks and troughs of about the same magnitude, with a rise in strontium at the edge of the otolith. This pattern can be interpreted as a warm early life history progressively cooling with the latter part of the fishes life being the coldest. In terms of depth this pattern could be interpreted as most of the fishes life having been spent in fairly shallow water, progressing to deeper water in the later part of its life. If strontium cycles are annual, then this fish would have been four to five years old with the last year spent in the coldest water.

The strontium surface of the otolith section of *Coryphaenoides mediterraneus* showed a minor sulcus peak in strontium. The nucleus was located in a pronounced peak following to lower values, before rising slightly, and then falling to yet lower values still. This pattern could be interpreted as showing the early life history to have been spent in cold water, and, surprisingly the rest of the life spent in going in two major steps into progressively warmer water. If the six or seven peaks in strontium along the nucleus to dorsal axis result from annual events then the fish appears to have spent up to two years in the initial cold water phase of its life going through each step of apparent warming in three and two years respectively. Examination of a broken section of the otolith showed no significant change in crystal widths that could be associated with its stepped appearance. We conclude that the changes in strontium reflects a progressive temperature change upwards.

The strontium surface of the otolith section of *Cetonurus globiceps* showed a major peak that could be interpreted as a sulcus peak. The rest of the otolith has a complex cycle of peaks and troughs but with only a weak tendency to decline in strontium content indicating a cyclical, but on average, similar environment over the life history of the fish. Broken sections of the otolith showed it to be characterised by very large crystals. It is possible that the physiology of otolith deposition in *C. globiceps* that results in such large crystals causes the otolith chemistry to become relatively insensitive to environmental input.

The strontium surface of the otolith sections of *Coryphaenoides leptolepis* showed a distinct sulcus peak, with cycling strontium levels going away from the nucleus to heightened strontium levels at the edge of the otolith. The strontium patterns of *Coryphaenoides leptolepis* suggest a life history similar to that of *Coryphaenoides armatus*.

The strontium surface of the otolith section of *Coelorincus labiatus* showed a distinct sulcus peak, with a complex strontium peak and trough structure without a distinctly heightened strontium edge. The pattern of strontium in the otolith of *C. labiatus* was intermediate between that of *C. globiceps*, and that of *Coryphaenoides armatus*.

The strontium surface of the otolith section of *Trachyrincus murrayi* showed a distinct sulcus peak. But otherwise showed a heightened central region corresponding to the early life history of the fish followed by a general lowering of strontium counts followed by an increase at the edge of the otolith. The strontium count of the otolith of *T. murrayi* showed affinities with the strontium count of the otolith of *Coryphaenoides mediterraneus*.

The strontium surface of the section of the otolith of *Antimora rostrata* showed three distinct peaks in the sulcus region. However, apart from a slightly depressed nucleus the strontium surface was more or less uniform, albeit cycling in a series of peaks and troughs.

Generally, the strontium patterns indicated similarities of life histories resulting in three groups:

Group I. *Coryphaenoides mediterraneus* and *Trachyrincus murrayi* showed similar patterns suggesting a cold early life with progressive warming interspersed with periods of cold.

Group II. *Coryphaenoides armatus* and *Coryphaenoides leptolepis* showed similar patterns suggesting a warmer early life with progressive cooling.

Group III. *Cetonura globiceps*, *Antimora rostrata* and *Coelorincus labiatus* showed similar patterns suggesting a uniform, albeit cycling, temperature over most of the life history of individuals.

While the Macrouridae are among the most successful families in their species richness and biomass on the continental slope and rise of the world ocean, relatively little is known about their early life-history. In the eastern North Atlantic, where the six species considered here were caught, alevins of only 26% of the 42 reported species are known (Merrett, 1986, 1989a). Among them are *Coryphaenoides leptolepis*, *C. mediterraneus*, *Coelorincus labiatus*. Free eggs of only six of the 300 or so species have been positively identified (Merrett, 1989b). Against this dearth of evidence, two patterns of development have been postulated, both derived by implication from what little is known. Marshall (1973) suggested a likely transient early life-history, with the eggs probably laid and fertilised near the bottom, developing as they rise under the buoyant influence of their oil globule. He considered that they would hatch close to the seasonal thermocline, before descending to their adult living depths. Merrett (1978) was inclined to substantiate this view when reporting midwater captures of alevins in mouth opening/closing nets in the eastern North Atlantic. However, in the light of near-bottom captures of alevins in opening/closing nets, and reports by Robertson (1981) that the ascent rate of buoyant eggs was retarded by the sculptured chorions found on macrourid eggs, on the other, Merrett (1989b) altered his views to consider his earlier observations as exceptional, rather than regular, occurrences. He conceded, however, that abyssal macrourids, due to their broad living area, might adopt a different

strategy to that necessary for the 'ribbon' distribution of slope dwelling species, so that either strategy might be employed depending on the spawning habitat of the species.

The current evidence suggesting three groupings of species based upon the differing implied temperature regimes experienced is not easy to reconcile fully with either hypothesis. It must be remembered that the vast majority of macrourids are demersal species and, while some have occasionally been taken well off the bottom (e.g. Stein, 1985), the bulk of their populations are evidently demersal (Merrett *et al.*, 1986). In addition, a 'smaller-shallower' distribution with the species' overall sounding range is known for at least *C. labiatus* and *C. armatus* in the group currently examined (Merrett *et al.*, 1990a). Against this must be set the known temperature regime at the capture sites of these fish (Fig. 13). From this, near surface development would involve alevins in initial relatively high environmental temperature, always followed by a sharp decrease as the juvenile descended to its living depth. Should near bottom development be the norm, then this trend would again hold true at least for the slope dwelling *C. labiatus*, although within a narrower range. Below 2000 m soundings, however, temperature variability is likely to be so low as to be undetectable, if development is demersal (Fig. 14). While it could be argued from the above that the continental rise and abyssal species of Group II might follow the Marshall (1973) development hypothesis and the slope species of Group III (excluding the morid, *A. rostrata*, about which nothing is known of its early life history) might take the Merrett (1989b) course of development, it is difficult to explain the evidence suggested by the Group I (slope) species early life-history pattern, on the basis of only temperature effects.

However, if temperature effects could be discounted, then metabolic effects may be responsible for the variation in otolith strontium in deep water fishes. Metabolic effects are likely to cause changes in the crystallisation rate of the otolith that appear as check rings (Campana, 1983; Gauldie and Radtke, 1990). The most obvious effect of metabolic change would be some kind of check, or mark, in the otolith caused by change in crystal size associated with pH change. Examination of deep water otoliths showed many such checks or marks, which, when grouped in the way that is usually done for age estimation, leads to a series of opaque zones with similar frequencies to the cycle of strontium changes observed in the otolith. However, similarity of frequencies still begs the question of what could drive a metabolic cycles if it wasn't temperature? Seasonal cycles have been reported from the biology of a wide range of deep-sea organisms (Tyler, 1988). Seasonal cycles associated with spawning are likely to involve changes in metabolic rate as energy requirements above that required for basal metabolism are acquired by increased predation rates. If changes in metabolic rates were sufficient to generate metabolic acidosis, then pH dependent changes in crystalline growth rate may be responsible for cycles in strontium. The small sizes of crystals in deep water fish otoliths suggests an alkaline endolympathic sac which may make the pH of the sac especially sensitive to decreases in pH.

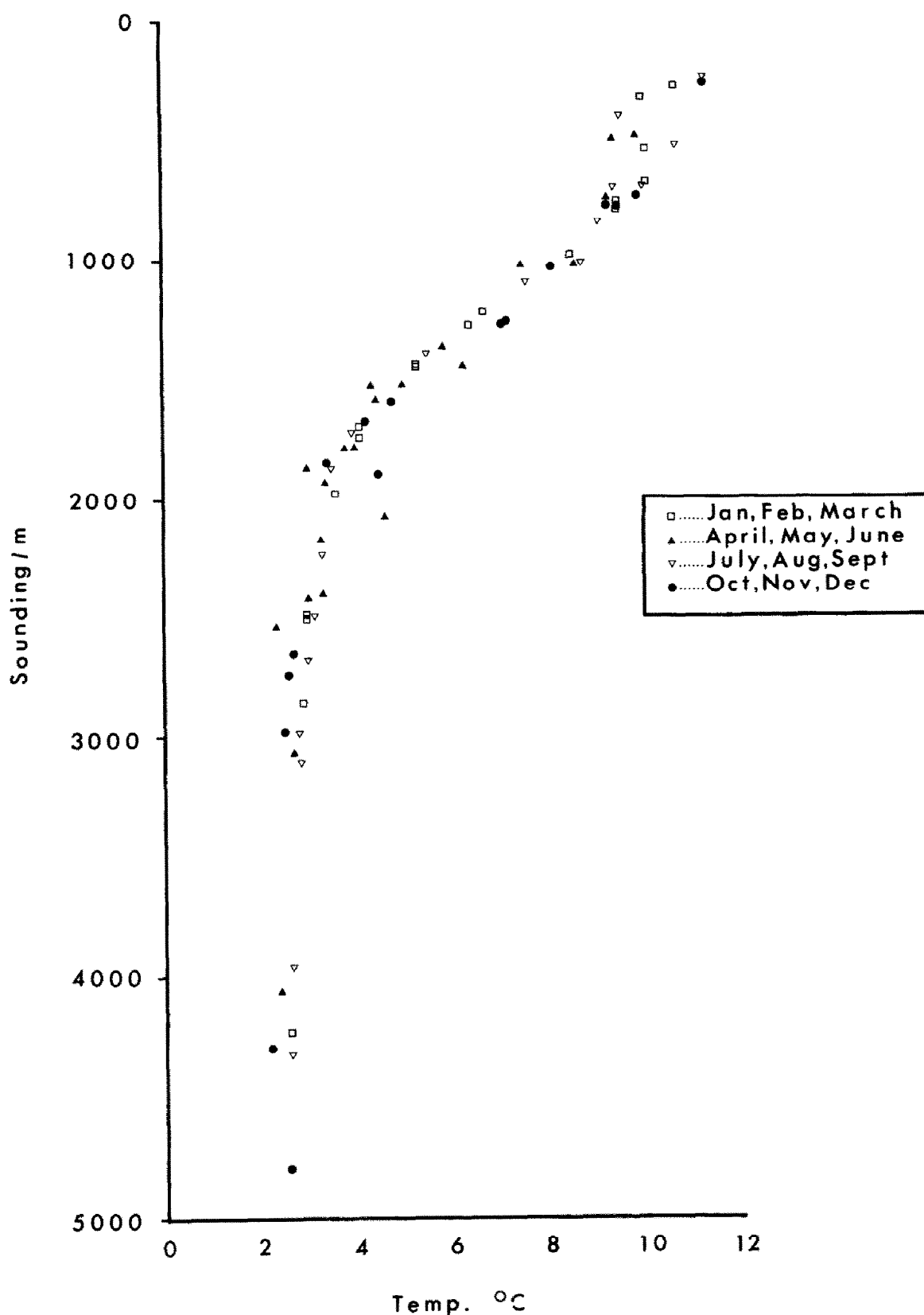


Fig. 14. Bottom water temperature is shown by depth and by season from a monitor mounted on the trawl door taken during sampling in the Porcupine Bight.

This alternative would mean that the groupings of fish by the patterns of their strontium cycles would now refer to their metabolic life histories rather than temperature life histories. In most fish species such a distinction would be practically impossible, but in the almost uniquely constant temperature deep water environment potential metabolic effects can be separated from the metabolism and non-metabolism effects of temperature.

The fossil otolith was clearly in another category. The high central peak was associated with apparent recrystallisation into block-like crystals that had occurred in the collapsed centre of the otolith. More detailed analysis (unpublished data) suggests that the collapsed core may be recrystallised aragonite and that the remainder of the otolith has apparently recrystallised as calcite. However, in comparison with deep water otoliths it is clear that when crystalline diagenesis occurs it is readily evident from inspection of the otolith. We conclude that there were no pressure related diagenetic effect occurring in the deep water otoliths that we have examined.

The age of deep water fishes presents a number of problems. Literal counting of check rings in the otolith can lead to impossibly high values. For example, Gordon and Duncan (1985) found up to 333 'age' marks in the otoliths of some deep water fishes. In addition, check rings in the orange roughy otolith show phase differences in mineralisation in different growth fields of the otolith that undermine the usefulness of check rings in age estimation (Gauldie, 1990). Strontium cycles appear in the otolith of the orange roughy otolith (Unpublished data), even though there is still a problem of metabolism/temperature effect because temperature variation at orange roughly depths (600–1000 m) is not likely to vary more than 1 or 2°C. The discrepancy between strontium peaks, and ageing 'marks' may be explained in the following way; the periodicity of strontium and calcium variation is not correlated with simple check ring periodicity in *Chrysophrys auratus* (Gauldie *et al.*, in preparation). However, reorganizing simple check ring variation into the kinds of groupings that are typically used in age estimation techniques may result in a match between check ring age and strontium periodicity. This effect is evident in the otoliths of *Coelorinchus labiata* and *Coryphaenoides leptolepis* in Table 1. Grouping check rings is not an uncommon procedure in developing age estimation techniques because ageing techniques often require agreed-upon conventions in order to establish what are to be accepted as annual, rather than spawning or simply 'accessory' checks in the otolith (Keir, 1960; Woodhead, 1968). Strontium cycles may provide a useful way of calibrating such ageing conventions for deep water fishes.

This survey has shown that elemental composition (particularly strontium) can vary in an environment in which temperatures are virtually constant. If our arguments about metabolic effects mimicking temperature effects are correct, such periodic variation may be driven by metabolic stanzas in the life of the fish. That kind of information would allow us to categorize fishes by the patterns of their individual life histories of categories that would reflect life histories which, in turn, could be used to subdivide

populations. The proportions of such categories in co-adapted communities could be expected to be fixed, or at least to vary stochastically, around some ideal target proportion. By definition, co-adapted communities must occur in some kind of regular proportionality. In contrast, random assemblages should show random distributions of individuals with different life-histories within species. Potentially, therefore, we have the means to settle the question of communities versus assemblages by appealing to the life history record of the otolith.

Acknowledgements—This research was partly supported by MAFFish, P. O. Box 297 Wellington, New Zealand; the British Natural History Museum, Cromwell Road, London; and by NSF grant Int-87-23084 made to Richard Radtke. This paper was written while R. W. G. was visiting Ichthyologist, Hawaii Institute of Geophysics, School of Ocean, Earth Sciences and Technology, University of Hawaii. SOEST contribution no. 2443.

REFERENCES

- Acker J. G., Byrne R. H., Ben-Yaakov S., Feely R. A. and Betzer P. R. (1987) The effect of pressure on aragonite dissolution rates in seawater. *Geochim. Cosmochim. Acta.* **51**, 2171–2175.
- Angel M. V. (1977) Windows into a sea of confusion: sampling limitations to the measurement of ecological parameters in oceanic mid-water environment. In: *Ocean Sound Scattering Prediction* (Edited by Anderson N. R. and Zahuranec B. J.), pp. 217–248. Marine Science 5, Plenum Press, New York.
- Beamish R. J. (1979) New information on the longevity of Pacific Ocean perch (*Sebastodes alutus*). *J. Fish. Res. Board Can.* **36**, 1395–1400.
- Berner R. A., Westrich J. T., Gruber R., Smith J. S. and Martens C. S. (1978) Dissolution kinetics of calcium carbonate in seawater IV. Theory of calcite dissolution. *Amer. J. Sci.* **274**, 108–135.
- Campana S. E. (1983) Calcium deposition and otolith check formation during periods of stress in coho salmon, *Oncorhynchus kisutch*. *Comp. Biochem. Physiol.* **75**, 215–220.
- Carriker M. R., Palmer R. E. and Prezant R. S. (1983) A crystallographic study of vertebrate otoliths. *Biol. Bull. (Woods Hole)* **125**, 441–463.
- Cleveland W. S. (1979) Robust locally weighted regression and smoothing scatterplots. *J. Am. Stat. Assoc.* **74**, 829–836.
- Coote G. E., Sparks R. J. and Blattner P. (1982) Nuclear microprobe measurement of fluorine concentration profiles with applications in archaeology and geology. *Nucl. Instrum. Meth.* **197**, 213–221.
- Crocket J. H. and Winchester J. W. (1966) Coprecipitation of zinc with calcium carbonate. *Geochim. Cosmochim. Acta.* **30**, 1093–1109.
- Davies N. M., Gauldie R. W., Crane S. A. and Thompson R. K. (1988) Otolith ultrastructure of smooth oreo, *Pseudocyttus maculatus*, and black oreo, *Allocyttus* sp., species. *Fish. Bull.* **86**, 499–515.
- Degens E. T., Deuser W. G. and Haedrich R. L. (1969) Molecular structure and composition of fish otoliths. *Mar. Biol.* **2**, 105–113.
- Dodd J. R. (1965) Environmental control of strontium and magnesium in *Mytilus*. *Geochim. Cosmochim. Acta.* **29**, 383–398.
- Fenton G. E., Ritz D. A. and Short S. A. (1990) $^{210}\text{Pb}/^{226}\text{Ra}$ disequilibrium in otoliths of blue grenadier, *Macruronus novaezealandiae*; problems associated with radiometric ageing. *Aust. J. Mar. Freshwater Res.* **41**, 467–473.

- Gauldie R. W. The information contained in abnormal fish otoliths. In preparation.
- Gauldie R. W. (1990) Phase differences between check rings locations in the orange roughy otolith. *Can. J. Fish. Aquat. Sci.* **47**, 760–765.
- Gauldie R. W. (1988a) The fine structure of check rings in the otolith of the New Zealand snapper (*Chrysophrys auratus*). *N.Z. J. Mar. Freshw. Res.* **22**, 273–278.
- Gauldie R. W. (1988b) Function, form and time-keeping properties of fish otoliths. *Comp. Physiol. Biochem.* **91**, 395–402.
- Gauldie R. W. (1987) The fine structure of check rings in the otolith of the Zealand orange roughy (*Hoplostethus atlanticus*). *N.Z. J. Mar. Freshw. Res.* **22**, 273–278.
- Gauldie R. W. and Radtke R. L. (1990) Microincrementation: facultative and obligatory precipitation of otolith crystal. *Comp. Biochem. Physiol.* **97A**, 137–144.
- Gauldie R. W. and Nelson D. G. A. (1990a) Otolith growth in fishes. *Comp. Biochem. Physiol.* **97A**, 119–135.
- Gauldie R. W. and Nelson D. G. A. (1990b) Interactions between crystal ultrastructure and microincrement layers in fish otoliths. *Comp. Biochem. Physiol.* **97A**, 447–459.
- Gauldie R. W. and Nelson D. G. A. (1988) Aragonite twinning and neuroprotein secretion are the cause of daily growth rings in fish otoliths. *Comp. Physiol. Biochem.* **90**, 501–509.
- Gauldie R. W., Mulligan K. P. and Thompson R. K. (1987) The otoliths of a chimaera, the New Zealand elephant fish *Callorhynchus miltii*. *N.Z. J. Mar. Freshw. Res.* **21**, 275–280.
- Gauldie R. W., Dunlop D. and Tse J. (1986) The remarkable lungfish otolith. *N.Z. J. Mar. Freshw. Res.* **20**, 81–92.
- Gauldie R. W., Graynoth E. J. and Ilingworth J. (1980) The relationship of the iron content of some fish otoliths to temperature. *Comp. Biochem. Physiol.* **66**, 19–24.
- Gauldie R. W., Coote G. C., Mulligan K. P. and West I. F. A chemical probe of the microstructural organisation of fish otoliths. (In preparation).
- Gauldie R. W., Davies N. M., Coote G. and Vickridge I. (1990) The relationship between organic material and check rings in fish otoliths. *Comp. Biochem. Physiol.* **97A**, 461–474.
- Gauldie R. W., Fournier D. A., Dunlop D. E. and Coote G. (1986) Atomic emission and proton microprobe studies of the ion content of otoliths of chinook salmon aimed at recovering the temperature life history of fishes. *Comp. Biochem. Physiol.* **73**, 21–29.
- Gauldie R. W., West I. F. and Davies N. M. (1989) K-selection characteristics of orange roughy (*Hoplostethus atlanticus*) stocks in New Zealand waters. *J. Appl. Ichthyol.* **5**, 127–140.
- Golovan G. A. (1978) Composition and distribution of the ichthyofauna of the continental slope off North-Western Africa. *Trudy Instituta Okeanologii* **111**, 195–258.
- Gordon J. D. M. and Duncan J. A. R. (1985) The ecology of the deep-seep benthic and benthopelagic fish on the slopes of the Rockall Trough, north eastern Atlantic. *Prog. Oceanog.* **15**, 37–69.
- Haedrich R. L. and Merrett N. R. Little evidence for faunal zonation or communities in deep sea demersal fish faunas. *Prog. Oceanog.* (In press).
- Haedrich R. L. and Merrett N. R. (1988) Summary atlas of deep-living demersal fishes in the North Atlantic Basin. *J. Nat. Hist.* **22**, 1325–1362.
- Hallam A. and Price N. B. (1968) Environmental and biochemical control of strontium in shells of *Cardium edule*. *Geochim. Cosmochim. Acta.* **32**, 319–328.
- Howell B. J., Baumgartner F. W., Bondi. K. and Rahn H. (1970) Acid-base balance as a function of body temperature. *Amer. J. Physiol.* **218**, 600–606.
- Hubbard J. I., Llinas R. and Quastel D. M. J. (1969) *Electrophysiological Analysis of Synaptic Transmission*. Edward Arnold, Ltd, London.
- Jethi R. K., Mackey M. G., Meredith P. D. and Wadkins C. L. (1972) Studies of the mechanisms of biological calcification III. The interaction of strontium with calcification matrix from beef tendon. *Calc. Tiss. Res.* **9**, 310–324.
- Johnson A. R., Armstrong W. D. and Singer L. (1968) The incorporation and removal of large amounts of strontium by physiologic mechanisms in mineralized tissues of the rat. *Calc. Tiss. Res.* **2**, 242–252.
- Jumars P. A. and Gallagher E. D. (1982) Deep-sea community structure: three plays on the benthic proscenium. In: *The Environment of the Deep Sea* (Edited by Ernst W. G. and Morin J. G.), pp. 217–255. Prentice Hall, Englewood Cliffs, New Jersey.
- Kalish J. M. (1989) Otolith microchemistry: validations of the effects of physiology, age, and environment on otolith composition. *J. Exp. Mar. Biol. Ecol.* **132**, 151–178.
- Katz A., Sass E., Starinsky A. and Holland H. D. (1972) Strontium behaviour in the aragonite–calcite transformation: an experimental study at 40–98°C. *Geochim. Cosmochim. Acta.* **36**, 481–496.
- Keir R. W. (1960) Answers to the questionnaire on age reading. ICNAF mimeographed document serial No. 714 (D.C.2), document No. 4, 67 pp.
- Kinsman D. J. J. and Holland H. D. (1969) The co-precipitation of cations with CaCO_3 –IV. The co-precipitation of Sr^{2+} with aragonite between 16 and 96°C. *Geochim. Cosmochim. Acta.* **33**, 1–17.
- Kshirsager S. G., Lloyd E and Vaughan J. (1966) Discrimination between strontium and calcium in bone and the transfer from blood to bone in the rabbit. *Br. J. Radiol.* **39**, 131–140.
- Laurs R. M., Nishimoto R. and Wetherall J. A. (1985) Frequency of increment formation on sagittae of North Pacific albacore (*Thunnus alalunga*). *Can. J. Fish. Aquat. Sci.* **42**, 1552–1555.
- Lehrman A. (1965) Strontium and magnesium in water and in *Crassostrea* calcite. *Science* **150**, 745–751.
- Li Y. H., Takahashi T. and Broecker W. S. (1969) Degree of saturation of CaCO_3 in the oceans. *J. Geophys. Res.* **74**, 5507–5525.
- Likens R. C., Bergh E. G. and Posner A. S. (1963) Comparative fixation of calcium and strontium by snail shell. *Am. N.Y. Acad. Sci.* **109**, 269–277.
- Lorens R. B. (1981) Sr, Cd, Mn and Co distribution coefficients in calcite as a function of calcite precipitation rate. *Geochim. Cosmochim. Acta.* **45**, 553–561.
- Lengemann F. W. (1960) Studies on the discrimination against strontium by bone growth *in vitro*. *J. Biol. Chem.* **235**, 1859–1862.
- Lowenstam H. A. (1964) Coexisting calcites and aragonites from skeletal carbonates of marine organisms and their strontium and magnesium contents. In: *Recent Researchers in the Fields of Hydrosphere, Atmosphere and Nuclear Chemistry*, pp. 373–404. Maruzen Co., Ltd, New York.
- Lowenstam H. A., Traub W. and Weiner S. (1984) *Nautilus* hard parts: a study of the mineral and organic constituents. *Paleobiology* **10**, 268–279.
- Marshall N. B. (1973) Family Macrouridae. In: *Fishes of the Western North Atlantic* (Edited by Cohen E. D.) Mem. Sears Fndn. Mar. Res., **1**, 496–537.
- Merrett N. R., Haedrich R. L., Gordon J. D. M. and Stehmann M. Deep demersal fish assemblage structure in the Porcupine Seabight (eastern North Atlantic): results of single warp trawling at lower slope to abyssal soundings. *J. Mar. Biol. Ass. U.K.* (In press).
- Merrett N. R., Gordon J. D. M., Stehmann M. and Haedrich R. L. Deep demersal fish assemblage structure in the Porcupine Seabight (eastern North Atlantic): slope sampling by three different trawls compared. *J. Mar. Biol. Ass. U.K.* (In press).
- Merrett N. R. (1989a) Fishing around in the dark. *New Scientist* **121**, 50–54.

- Merrett N. R. (1989b) The elusive macrourid alevin and its seeming lack of potential in contributing to intrafamilial systematics. In: *Papers on the Systematics of Gadiform Fishes* (Edited by Cohen D. M.), pp. 175-185. Los Angeles Co. Nat. Hist. Mus. Sci. Ser., 32, pp. 262.
- Merrett N. R. (1987) A zone of faunal change in assemblages of abyssal demersal fish in the eastern North Atlantic: a response to seasonality in production? *Biol. Oceanog.* **5**, 137-151.
- Merrett N. R. (1986) Macrouridae of the eastern North Atlantic. *Fiche d'Identification du Plancton*. 173/174/175, pp. 11.
- Merrett N. R., Badcock J., Ehrich S. and Hulley P. A. (1986) Preliminary observations on the near-bottom ichthyofauna of the Rockall Trough: a contemporaneous investigation using commercial-sized midwater and demersal trawls to 1000 m depth. *Proc. Roy. Soc. Edinb.* **88B**, 312-314.
- Merrett N. R. (1978) On the identity and pelagic occurrence of larval and juvenile stages of rattail fishes (Family Macrouridae) from 60°N, 20°W and 53°N, 20°W. *Deep-Sea Res.* **25**, 147-160.
- Milliman J. D. (1974) *Marine Carbonates*. Springer, Berlin.
- Morales-Nin B. (1987) Ultrastructure of the organic and inorganic constituents of the sea bass. In: *Age and Growth of Fish* (Edited by Summerfelt R. C. and Hall G. E.), pp 331-344. Iowa State University Press, Ames, Iowa.
- Morales-Nin B. (1986) Chemical composition of the otoliths of the sea-bass (*Dicentrarchus labrax* Linnaeus, 1758) *Pisces, Serranidae*. *Cybium* **10**, 115-120.
- Morse J. W. and MacKenzie F. T. (1990) *Geochemistry of Sedimentary Carbonates. Developments in Sedimentology* 48. Elsevier, Amsterdam.
- Mucci A. and Morse J. W. (1983) The incorporation of Mg^{2+} and Sr^{2+} into calcite overgrowths: influences of growth rate and solution composition. *Geochim. Cosmochim. Acta* **47**, 217-233.
- Mugiya Y. and Uchimura T. (1989) Otolith resorption by anaerobic stress in the goldfish, *Carassius auratus*. *J. Fish Biol.* **35**, 813-818.
- Mugiya Y. (1987) Phase difference between calcification and organic matrix formation in the diurnal growth of otoliths in the rainbow trout, *Salmo gairdneri*. *Fish. Bull.* **35**, 395-401.
- Mugiya Y. (1966) Calcification in fish and shell-fish XI. Seasonal changes in calcium and magnesium concentration of the otolith fluid in some fish, with special reference to the zone of formation of their otolith. *Bull. Jpn. Soc. Sci. Fish.* **32**, 549-557.
- Mulligan K. P., Gauldie R. W. and Thomson R. (1990) Otoconia from four New Zealand Chimaeriformes. *Fish. Bull.* **87**, 923-934.
- Mulligan K. P. and Gauldie R. W. (1989) The biological significance of the variation in crystalline morph and habit of otoconia in elasmobranchs. *Copeia* **1989**, 856-871.
- Netter H. (1969) *Theoretical Biochemistry*. Oliver and Boyd, Edinburgh.
- Neuman W. F., Bjornerstedt R. and Mulryan B. J. (1963) Synthetic hydroxyapatite crystals II. Aging and strontium incorporation. *Arch. Biochem. Biophys.* **101**, 215-224.
- Neville H. C. (1967) Daily growth layers in animals and plants. *Biol. Rev.* **42**, 421-441.
- Odum H. T. (1957) Biochemical deposition of strontium. *Texas University Institute of Marine Science* **4**, 39-114.
- Opel I. L. and Judd J. M. (1967) Skeletal distribution of strontium and calcium and strontium/calcium ratios in several species of fish. In: *Strontium Metabolism* (Edited by Lenihan J. M. A., Loutit J. F. and Martin J. H.), pp. 103-109. Academic Press, New York.
- Oxburgh H. M., Seguit R. E. and Holland H. D. (1959) Coprecipitation of Sr with calcium carbonate from aqueous solutions. *Geol. Soc. Am. Abs.* **60**, 1653-1654.
- Pannella G. (1980) Growth patterns in fish sagittae. In: *Skeletal Growth of Quatic Organisms* (Edited by Rhoads D. C. and Lutz R. A.), pp. 519-560. Plenum Press, New York.
- Pannella G. (1971) Fish otoliths: daily growth layers and periodical patterns. *Science* **174**, 1124-1126.
- Pilkey O. H. and Goodell H. G. (1963) Trace elements in recent mollusc shells. *Limnol. Oceanog.* **8**, 137-148.
- Pilkey O. H. and Hower J. (1960) The effect of the environment on the concentration of skeletal magnesium and strontium in *Dendraster*. *J. Geol.* **68**, 203-216.
- Plummer L. N. and Busenberg E. (1987) Thermodynamics of aragonite-strontianite solid solution: results from stoichiometric solubility at 25 and 76°C. *Geochim. Cosmochim. Acta* **51**, 1393-1411.
- Porzig H. (1981) Transmembrane strontium movements and strontium-induced changes in membrane cation permeability in non-excitable cell membranes. In: *Handbook of Stable Strontium* (Edited by Skoryna S. C.). Plenum Press, New York.
- Posner A. S. (1969) Crystal chemistry of bone mineral. *Physiol. Rev.* **49**, 760-792.
- Pulfrich A. and Griffiths C. L. (1988) Growth, sexual maturity and reproduction in the hottentot *Pachymetopon blochii* (Val.). *S. Afr. J. Mar. Sci.* **7**, 25-36.
- Radtke R. L., Townsend D. W., Folsom S. D. and Morrison M. A. (1989) Strontium; calcium concentration ratios in otoliths of herring larvae as indicators of environmental histories. *Env. Biol. Fish.* **27**, 51-61.
- Radtke R. L., Fine M. L. and Bell J. (1985) Somatic and otolith growth in the oyster toadfish (*Opsanus tau* L.). *J. Exp. Mar. Biol. Ecol.* **90**, 259-275.
- Radtke R. L. (1984) Codfish otoliths: information storage structures. *Floedvigen Rapportser* **1**, 273-298.
- Ralston S. and Williams H. A. (1988) Depth distributions, growth and mortality of deep-slope fishes from the Mariana Archipelago, U.S. NOAA-TM-NMFS-SWFC Tech. Man. **113**, 47.
- Ralston S. and Miyamoto G. T. (1983) Analyzing the width of daily growth rings of otoliths. *Fish Bull.* **74**, 990-994.
- Rannou M. and Thiriot-Quievreux G. (1975) Structure des otoliths d'un Macrouridae (Poisson Gadiforme) bathyal. Etude au microscope electronique a balayage. *Ann. Inst. Oceanog. Paris* **51**, 195-201.
- Robertson D. A. (1981) Possible functions of surface structure and size in some planktonic eggs of marine fishes. *N.Z. J. Mar. Freshw. Res.* **15**, 147-153.
- Rosenthal H. L. (1981) Content of stable strontium in man and animal biota. In: *Handbook of Stable Strontium*, (Edited by Skoryna S. C.). Plenum Press, New York.
- Saunders R. L. (1963) Respiration of the Atlantic cod. *J. Fish. Res. Bd Canada* **20**, 373-386.
- Six L. D. and Horton H. F. (1977) Analysis of age determination methods for yellowtail rockfish, canary rockfish and black rockfish of Oregon. *Fish. Bull.* **75**, 405-414.
- Smith K. L. (1978) Metabolism of the abyssopelagic rattail *Coryphaenoids auratus* measured *in situ*. *Nature* **274**, 362-364.
- Sonderegger J. L., Brower K. R. and Lefebvre V. G. (1976) A preliminary investigation of strontianite dissolution kinetics. *Am. J. Sci.* **276**, 997-1022.
- Speer J. A. (1983) Crystal chemistry and phases relations of orthorhombic carbonates. In: *Reviews in Mineralogy, Carbonates-Mineralogy and Chemistry* (Edited by Reeder R. J.), pp. 145-189. Mineralogical Society of America. Bookcrafters, Inc., Chelsea, MI.
- Stein D. L. (1985) Towing large nets by single warp at abyssal depths: methods and biological results. *Deep Sea Res.* **32**, 183-200.
- Storey E. and West V. C. (1971) Factors modifying Ca/Sr discrimination by bone and synthetic apatite minerals *in vitro*. *Calc. Tiss. Res.* **6**, 290-300.

- Strong M. B., Neilson J. D. and Hunt J. J. (1986) Aberrant crystallisation of pollock (*Pollachius virens*) otoliths. *Can. J. Fish. Aquat. Sci.* **43**, 1457–1463.
- Suess E. and Fütterer D. (1972) Argonitic ooids: experimental precipitation from seawater in the presence of humic acid. *Sedimentology* **19**, 129–139.
- Sverdrup H. W., Johnson M. W. and Fleming R. H. (1942) *The Oceans, Their Physics, Chemistry and General Biology*. Prentice-Hall, Englewood Cliffs, New Jersey.
- Swan E. F. (1957) The meaning of strontium–calcium ratios. *Deep Sea Res.* **4**, 71.
- Townsend D. W., Radtke R. L., Morrison M. A. and Folsom S. D. (1989) Recruitment implications of larval herring over wintering distributions in the Gulf of Maine inferred using a new otolith technique. *Mar. Ecol. Prog. Ser.* **55**, 1–13.
- Tyler P. A. (1988) Seasonality in the deep sea. *Oceanogr. Mar. Biol. Annu. Rev.* **26**, 227–288.
- Weiner S. and Traub W. (1984) macromolecules in mollusc shells and their functions in biomineralization. *Phil. Trans. Roy. Soc., Lond., Ser. B* **304**, 425–434.
- Wilber K. M. and Saleuddin A. S. M. (1983) Shell formation. In: *The Mollusca*, Vol. 4, *Physiology*, Part I (Edited by Saleuddin A. S. M. and Wilber K. M.), pp. 236–288. Academic Press, New York.
- Woodhead P. M. J. (1968) Seasonal changes in the calcium content of the blood of Arctic cod. *J. Mar. Biol. Ass. O.K.* **48**, 81–91.
- Zeller E. J. and Wang J. (1956) Factors influencing precipitation of calcium carbonate. *Bull. Am. Ass. Petrol. Geol.* **40**, 140–152.